A statistical approach to quasi-extinction forecasting

E. E. Holmes[1,4], J. L. Sabo[2], S. V. Visicido[1], and W. F. Fagan[3]

1. **Northwest Fisheries Science Center, 2725 Montlake Boulevard East, Seattle, WA 98112**
2. **School of Life Sciences, Arizona State University, Tempe, AZ**
3. **Dept. of Biology, University of Maryland, College Park, MD 20742**
4. **To whom correspondence should be addressed**

Abstract

Forecasting population decline to critical thresholds (quasi-extinction risk) is one of the central objectives in population viability analysis (PVA) and figures prominently in the criteria used by major conservation organizations for ranking species. In this paper, we argue that forecasting quasi-extinction risk does not necessarily hinge on knowing the biological details underlying the population dynamics. The stochastic and multiplicative nature of population growth means that the ensemble behavior of population trajectories converges to common statistical forms across a wide variety of stochastic population processes. In this paper, we provide a theoretical basis for this argument, showing how a variety of complex stochastic population processes (including age-structured, metapopulation, and density-dependent) can be approximated by a simple stochastic approximation: the stochastic exponential growth process overlaid with random Gaussian errors (CSEG). We use both simulated and real data to show that with 20 to 30 years of data, a CSEG model can be estimated that accurately approximates quasi-extinction patterns. The simulated data are derived from some of the noisiest population processes (density-dependent feedback, interspecies interactions, and strong age-structure cycling); yet even for these noisy data, we found that with at least 20 years for parameterization the 95% confidence intervals on the quasi-extinction estimates are much less than the full range of 0 to 1. One of the strengths of an approach using theoretically derived statistical models is that the parameter uncertainties can be properly specified in a traditional statistical manner, and the confidence intervals have traditional statistical interpretations – unlike the *ad hoc* uncertainties presented in many PVAs. Thus, we argue that meaningful estimates of quasi-extinction risk are possible even with relatively noisy, albeit not short, datasets. The existence of

parameter-sparse statistical approximations suggests that the key issue is robust parameter estimation, rather than any real unpredictability of the quasi-extinction risk itself.

Keywords: Stochastic models, stochastic estimation, population models, population viability analysis, extinction analysis

"…a typical random mass phenomenon, unpredictable in certain details, predictable in certain numerical proportions of the whole."

— George Polya (1968), 'Mathematics and Plausible Reasoning'

Introduction

Population models are a standard tool in both academic ecology and conservation science; however, the goals of population models in these two arenas are notably different. In academic ecology, one typically uses population models to infer the biological mechanisms underlying a given set of population data. In conservation science, one constructs a population model to forecast future trends based on recent population data; this approach is referred to as population viability analysis, or PVA (Boyce 1992; Beissinger & McCullough 2002; Morris & Doak 2003). The key distinction is that while academic efforts typically focus on the causes of population dynamics, conservation science attempts to predict their consequences.

In both endeavors, published research has made increasing use of parameter-rich, mechanistic models. This approach to PVA forecasting has a number of significant pitfalls. Most importantly, a mechanistic model can only be specified with detailed and abundant data. Such data are typically not available for the populations of concern to conservationists (Morris *et al.* 2002; DeMaster *et al.* 2004). Even when some detailed data are available (e.g., age-specific survivorship or fecundity), they typically cover too short a duration to specify the annual variability of the model parameters. The result is that either annual variability is not incorporated into the model, or that some annual variability must be assumed using (hopefully) plausible parameters. Then there is the problem of determining the uncertainty in the model parameters. Since many parameters are specified rather than estimated from the data, we cannot

estimate their uncertainty using traditional statistical methods. At best, we can perform some type of sensitivity analysis. Because of these basic limitations of the data, managers and policy-makers who are charged with forecasting populations often recommend against quantitative PVAs (DeMaster et al. 2004).

In this paper, we argue for a different approach to forecasting, one based on the convergent random mass properties of stochastic population dynamics. Random mass properties refer to the emergent properties in a large sample of replicates from some unknown stochastic process. As Polya notes in the opening quote, random mass properties can be predictable even when the details of the underlying process are unpredictable and/or unknown. Inference based on the random mass properties of population trajectories is very different, both philosophically and practically, from inference based on a mechanistic model (Figure 1a). The latter type of inference is the fashion in PVA, while the former is the foundation of classical statistical inference.

To illustrate reasoning using random mass properties, we will first walk though a well-worn example from statistics: the inference of large sample means (Figure 1b). Regardless of the underlying data distribution, the Central Limit Theorem (CLT) shows that the distribution of the large-sample mean is always normal as the sample size n grows. The normal distribution is a convergent mass property, meaning that although the process that generated the data is unknown, the distribution of large sample means is known. Once the existence of a convergent mass property has been determined, we need to estimate it from a finite sample. The CLT again guides us here, showing that there is a common relationship between certain properties of small samples and the parameters of the limiting normal distribution. This allows estimation of the large sample mean distribution from small samples.

Our goal is to extend this type of reasoning to the estimation of a specific random mass property of stochastic population trajectories: the probability of decline below a pre-defined threshold. Since this metric does not measure absolute extinction *per se*, we instead use the term quasi-extinction (Morris & Doak 2003). We focus exclusively on quasi-extinction thresholds that are above the level at which demographic stochasticity and Allee effects become important. These factors accelerate the decline toward absolute extinction making it differ in fundamental ways from the decline to a critical threshold (Lande *et al.* 2003; Fagan & Holmes 2006). Quasi-extinction probabilities are an important risk metric used in policy arenas. The World Conservation Union's IUCN risk criteria (Mace & Lande 1991) and the proposed quantitative criteria for the U.S. Endangered Species Act (DeMaster et al. 2004), for example, both explicitly rely on quasi-extinction probabilities.

The estimation of quasi-extinction risk using convergent random mass properties involves synthesizing two bodies of theoretical research (Figure 1c): the theory of population trajectories and their random mass properties, and the estimation of stochastic models from short time series. We begin by integrating multiple avenues of theoretical work to illustrate the range of stochastic population models that can be approximated by a stochastic exponential process overlaid with Gaussian errors. It turns out that populations with both density-independent and density-dependent dynamics can be approximated by this type of parameter-sparse random walk. The quasi-extinction properties of this simple approximation are similar to those of more complex, parameter-rich processes, but the approximation depends on only three parameters. After reviewing the theoretical basis for these approximations, we present two cross-validation studies of quasi-extinction forecasts. The first is based on simulations of three types of cyclic population processes, and the second is based on analysis of a large database of time series from

species of concern to conservationists. We conclude with a discussion of the merits of simple stochastic approximations in conservation risk analysis, *vis-à-vis* the important criticisms that have been raised against PVA models.

Random mass models for quasi-extinction

The quasi-extinction probability is the fraction of population trajectories that cross below a specified threshold within a particular time horizon or forecast length (Figure 2a). The quasi-extinction probability is a smooth function of the threshold and horizon, which can be displayed as a 3-dimensional surface (Figure 2b). In this paper, we will work with slices of this surface – either the probability of hitting a particular threshold across different forecast lengths (Figure 2c) or the probability of hitting a range of different thresholds within a particular forecast length (Figure 2d). Our goal is to identify a simple stochastic model that approximates these patterns of quasi-extinction risk across broad classes of population processes.

In this paper, we focus on forecasting expected probabilities

$$\mathrm{E}[Pr(qe)] = \int_x P(\{...., x_{-2}, x_{-1}, x_0\})\, P(qe \text{ in } \{x_1, x_2, ..., x_T\} \mid \{...x_{-2}, x_{-1}, x_0\}), \qquad [1]$$

where *qe* is shorthand for quasi-extinction. In this equation, $\{...x_{-2}, x_{-1}, x_0\}$ are the past (observed) population trajectories and $\{x_1, x_2, ..., x_T\}$ are the population counts within a particular forecast of length *T*. $P(\{...., x_{-2}, x_{-1}, x_0\})$ is the probability of the 'past' and $P(qe \mid \{...., x_{-2}, x_{-1}, x_0\})$ is the probability of 'future quasi-extinction' given the past. To calculate the expected quasi-extinction probability, we integrate over the set of all possible past trajectories. E[*Pr*(*qe*)] is then the average probability of quasi-extinction observed by selecting

time series randomly from the set of possible past trajectories, and measures the propensity of the process for quasi-extinction.

Random mass properties of density-independent population processes

Theoretical results on density-independent population processes are based on the study of simple random walks. A simple random walk starts at some Y_t and at each time step takes a random hop to Y_{t+1}: $Y_{t+1} = Y_t + \xi$, where the hop length ξ is a random variable. Our starting point for population modeling is a particular random hop model, in this case the stochastic exponential growth model (Lewontin & Cohen 1969):

$$\log N_{t+1} = \log N_t + \mu + \eta_t \qquad [2]$$

Sample trajectories for this type of process are shown in Figure 2a. The mean population growth rate is μ and the η_t are the year-to-year deviations from that mean. In this model, the deviations might be drawn from any distribution with mean zero and variance σ_p^2.

Two defining characteristics of linear random walks (like Eq. 1 or 2) are (1) that the mean and variance of $\log N_{t+\tau}/N_t$ scale linearly with τ (Figure 2b), and (2) that $\log N_{t+\tau}/N_t$ has a normal distribution for large τ (Figure 2c). Consequently, no matter what is the distribution of the errors (the η_t's) in Eq. 2, a stochastic exponential growth model with Gaussian errors emerges as τ gets large (Feller 1968):

$$\log N_{t+\tau} = \log N_t + \mu + \varepsilon_t, \qquad [3]$$

where ε is drawn from a normal distribution with mean zero and variance σ_p^2. We will refer to this as the SEG model, which stands for Stochastic Exponential growth with Gaussian errors. This model will appear repeatedly in the discussions to follow. An analytical solution to the

quasi-extinction surface of the SEG model can be specified using its diffusion approximation (Lande & Orzack 1988; Dennis *et al.* 1991):

$$d(\log N)_t = \mu dt + \sigma_p dW_t, \qquad [4]$$

where W_t is the Weiner process, also known as Brownian motion.

The SEG is the asymptotic stochastic approximation for several important classes of population models. The first is the class of stochastic, age-structured population models with no density dependence:

$$\begin{bmatrix} N_{1,t+\tau} \\ N_{2,t+\tau} \\ N_{3,t+\tau} \\ \vdots \\ N_{k,t+\tau} \end{bmatrix} = \mathbf{A}_t \begin{bmatrix} N_{1,t} \\ N_{2,t} \\ N_{3,t} \\ \vdots \\ N_{k,t} \end{bmatrix}. \qquad [5]$$

$\mathbf{A}_t$ is the stochastic transition matrix for time t and generally looks something like

$$\mathbf{A}_t = \begin{bmatrix} f_{1,t} & f_{2,t} & f_{3,t} & \cdots & f_{k,t} \\ s_{1,t} & 0 & 0 & \cdots & 0 \\ 0 & s_{2,t} & 0 & \cdots & 0 \\ 0 & 0 & s_{3,t} & \cdots & 0 \\ 0 & 0 & 0 & \cdots & 0 \end{bmatrix}. \qquad [6]$$

The *f*'s and *s*'s are age-specific fecundities and survival rates at time *t*, and are random variables. As long as the distributions of *f* and *s* are reasonably smooth and do not change systematically over time, any weighted sum $N_t = \sum_i w_i N_{i,t}$ can be approximated by the SEG model at large τ (Tuljapurkar & Orzack 1980; Tuljapurkar 1989; Caswell 2000). This will be true regardless of the specific distributions adopted or any temporal correlations among the parameters.

Figure 3 shows an example. This shows a SEG approximation to a Chinook salmon population (*Oncorhynchus tshawytscha)*, following Holmes (2004). The model has five classes: individuals aged 1 to 4 years, plus returning spawners. The stochastic transition matrix is

$$\mathbf{A}_t = \begin{bmatrix} 0 & 0 & 0 & 0 & ps_1 m\varepsilon_{1,t} \\ s_2\varepsilon_{2,t} & 0 & 0 & 0 & 0 \\ 0 & s_o\varepsilon_{3,t} & 0 & 0 & 0 \\ 0 & 0 & (1-b_4)s_o\varepsilon_{4,t} & 0 & 0 \\ 0 & 0 & b_4 s_o\varepsilon_{4,t} & b_5 s_o\varepsilon_{5,t} & 0 \end{bmatrix}, \qquad [7]$$

where s_i is the age-specific survival, b_i is the fraction of class i (= 4 or 5) that enters the spawner class, m is the average female fecundity, p is the probability of survival during migration, and $\varepsilon_{i,t}$ is the year-to-year variability. Figure 3a shows a collection of 50-year time series for the total population size simulated with this model (the caption gives values for the parameters). In this illustrative example, the total population at each time step was specified as $N_t = \sum_i w_i N_{i,t}$, where w_i is the reproductive value of age i. The SEG approximation often works much better with this type of weighting. Each simulation was run for 100 years before we began plotting the 50-year trajectories; this is a simple numerical method for starting each simulation at a randomly selected point from the stochastic equilibrium.

The total population counts from this age-structured process show all the key statistical patterns of a SEG process. The mean and variance of $\log N_{t+\tau}/N_t$ scale linearly with τ, and the variance passes through the origin as expected (Figure 3b). The long-term distributions $\log N_{10}/N_0$ and $\log N_{50}/N_0$ both have an approximately normal distribution (Figures 3c,d). An appropriate SEG for this example can be specified from plots of the mean and variance as a function of τ (Figure 3b), and Figures 3e,f show that this two-parameter SEG model closely approximates the quasi-extinction surface of the salmon population trajectories. SEG

approximations for a variety of other structured population processes are shown in Tuljapurkar and Orzack (1980), Caswell (2000), Holmes (2001), Morris and Doak (2003), and Holmes (2004).

A second important class of stochastic models for which the SEG is a good asymptotic approximation is the class of metapopulation models with continuous, density-independent dynamics (Holmes & Semmens 2004). In this model, each local population *i* has its own stochastic local growth function as well as a stochastic dispersal function describing migration to and from other populations:

$$\begin{aligned} N_{i,t+1} &= \text{growth - dispersal out + dispersal in} \\ &= N_{i,t}e^{z_{i,t}} - d_{i,t}N_{i,t}e^{z_{i,t}} + \sum_{j\neq i}\alpha_{ji,t}d_{j,t}\ N_{j,t}e^{z_{j,t}} \end{aligned} \qquad [8]$$

where $z_{i,t}$ is the stochastic growth of local population *i* in year *t* and can be drawn from any smooth statistical distribution. Some fraction $d_{i,t}$ of individuals emigrates from local population *i* at year *t* (and similarly $d_{j,t}$ individuals emigrate from local population *j*). The rate of immigration into local population *i* is given by summing the fractions $\alpha_{ji,t}$ of dispersers from each of the other populations *j*. No constraints need be placed on the distributions of the growth and dispersal parameters (the *z*'s, *d*'s, and α's) or their temporal correlations. Equation 8 is quite general, allowing some sites to be sources ($z_i > 0$), sinks ($z_i < 0$), dispersal sources, or dispersal targets. It can be used to model any spatial pattern of dispersal, any system of (spatially or temporally) correlated local growth rates, and any combination or pattern of patch sizes. Large patches can be created by specifying a collection of local populations with full dispersal between them. The model also allows for some anisotropy in the dispersal, as long as all sites are connected to some degree to ensure that the transition matrix **A** (in Eq. 10) is ergodic.

This metapopulation model can be written succinctly as

$$\begin{bmatrix} N_{1,t+1} \\ N_{2,t+1} \\ N_{3,t+1} \\ \cdots \\ N_{k,t+1} \end{bmatrix} = \mathbf{A}_t \begin{bmatrix} N_{1,t} \\ N_{2,t} \\ N_{3,t} \\ \cdots \\ N_{k,t} \end{bmatrix}. \qquad [9]$$

In this model, the matrix $\mathbf{A}_t$ encapsulates both dispersal and local growth:

$$\mathbf{A}_t = \begin{bmatrix} (1-d_1)e^{z_1} & \alpha_{21}d_2e^{z_2} & \alpha_{31}d_3e^{z_3} & \cdots & \alpha_{k1}d_ke^{z_k} \\ \alpha_{12}d_1e^{z_1} & (1-d_2)e^{z_2} & \alpha_{32}d_3e^{z_3} & \cdots & \alpha_{k2}d_ke^{z_k} \\ \alpha_{13}d_1e^{z_1} & \alpha_{23}d_2e^{z_2} & (1-d_3)e^{z_3} & \cdots & \alpha_{k3}d_ke^{z_k} \\ \cdots & \cdots & \cdots & \cdots & \cdots \\ \alpha_{1k}d_1e^{z_1} & \alpha_{2k}d_2e^{z_2} & \alpha_{3k}d_3e^{z_3} & \cdots & (1-d_k)e^{z_k} \end{bmatrix}. \qquad [10]$$

The *t* subscripts on the *d*'s, α's, and *z*'s have been dropped to remove clutter; the subscript on the matrix symbol reminds us that its elements are time-dependent.

A projection of this model forward in time results in a product of ergodic random matrices (the $\mathbf{A}_t$'s). This metapopulation model thus falls into a class of stochastic models whose random mass properties have been well studied (Furstenberg & Kesten 1960). Existing theoretical work shows that the logarithm of the total metapopulation size, $\log M_{t+\tau} = \log \sum N_{i,t+\tau}$, will be asymptotically normal, with a variance and mean that scale linearly with τ (Holmes & Semmens 2004):

$$\log M_{t+\tau} / M_t \underset{t\to\infty}{\rightarrow} \text{normal}(\tau\mu_m, \tau\sigma_m^2). \qquad [11]$$

Again, these are the key properties of an SEG model. Figure 4 shows the SEG approximation for quasi-extinction risk in a simulation of this model with 49 heterogeneous sites connected by directional dispersal rates (of 5-25% per year). The sites had different propensities to produce dispersers, and different local growth rates.

In the SEG there is only one type of variance affecting $\log N_{t+\tau}/N_t$: the variance in which one random fluctuation builds upon the last and the variance in $\log N_{t+\tau}/N_t$ continually grows as τ increases. In population modeling, this type of variability is termed *process error*. There is another type of variability, termed *non-process error*, which does not feed into the next year. In this case the population counts, called O_t for observed counts, appear to be produced by an unseen underlying process N_t that is overlaid with an independent source of variability:

$$\begin{aligned} O_t &= N_t + \varepsilon_{np,t} \\ O_{t+\tau} &= N_t + \varepsilon_{np,t+\tau} \end{aligned} \qquad [12]$$

Non-process error typically arises from some internal feedback in the dynamics that causes periodicity. This type of variability does not continually grow as τ increases.

If we combine the SEG with a pure non-process error model (Eq. 12), we obtain a corrupted stochastic exponential with Gaussian errors (CSEG):

$$\log N_{t+1} = \log N_t + \mu + \varepsilon_{p,t} \qquad [13a]$$

$$\log O_{t+1} = \log N_{t+1} + \varepsilon_{np,t+1}. \qquad [13b]$$

The N_t represent an unobserved population dynamic driven only by process error. The process error $\varepsilon_{p,t}$ is a normally distributed variable with mean zero and variance σ_p^2 -- like for the SEG, this normality arises due to the multiplicative nature of process errors. The O_t are the observed counts corrupted with non-process error. For this paper, we approximate these errors using a normal distribution with mean 0 and variance σ_{np}^2; the non-process errors produced by common types of population feedbacks are often normal or quasi-normal although decidedly non-normal cases also exist.

The CSEG is a three-parameter model with all the properties of a SEG (Eq. 13a) as well as the properties of a pure Gaussian error process (Eq. 13b). The mean of log $O_{t+\tau}/O_t$ scales linearly with τ, like a SEG. If μ equals zero, however, the mean of log $O_{t+\tau}/O_t$ is zero, like a pure Gaussian error process. The variance of log $O_{t+\tau}/O_t$ scales linearly with τ in both cases, due to the process error variance in the SEG portion. Unlike the SEG, however, the variance has a non-zero intercept due to the non-process error. Finally, the distribution of log $O_{t+\tau}/O_t$ in the CSEG is normal for large τ just as in the SEG case. In the following sections, we discuss two common population dynamics that result in non-process error variability, and illustrate how a CSEG can approximate their quasi-extinction probabilities.

Random mass properties of age- or stage-specific counts

A stochastic age-structured process does not asymptotically approach a single stable age distribution. Convergence to a single stable age structure is prevented because the age structure has an inherent tendency to cycle, and random perturbations continuously trigger these cycles. Instead, the age structure enters a *stochastic equilibrium*, which is a bounded set of age structures within which the current age structure wanders. The number of individuals at age *i* thus fluctuates about some mean value, and those fluctuations turn out to be normally distributed (Tuljapurkar & Orzack 1980; Tuljapurkar 1989). When we follow the total population (as in the previous section), we average over these fluctuations. If we are interested in the quasi-extinction properties of a particular age, however, or when the available data are restricted to a particular age, the age-structure fluctuations introduce a large non-process error and the SEG approximation cannot be used.

Spawner counts from the Chinook salmon model (Eq. 7) provide an example of this problem. Although the spawner count ($N_{5,t}$) tracks the overall total population trend, the life history of this species also produces strong spawner cycles (Figure 5a). When the variance in $\log N_{5,t+\tau}/N_{5,t}$ is plotted versus τ (Figure 5b), we see the same linear trend displayed by the total population (Figure 3b) but with a non-zero intercept due to the spawner cycles. The distribution of $\log N_{5,t+\tau}/N_{5,t}$ is approximately normal for large τ (Figure 5c,d), as predicted by theory. The random mass properties of the log spawner counts are thus the same as those of a CSEG, and Figures 5e and 5f show that the CSEG model successfully describes their quasi-extinction probabilities across different threshold levels and forecast lengths. More examples of CSEG approximations for the age-specific counts of sea turtles, petrels, and other salmonids can be found in works by Holmes (2001; 2004).

Random mass properties of density-dependent population processes

A myriad of natural forces can lead to density dependence, and ultimately to population regulation. A regulated stochastic population process differs in several fundamental ways from a density-independent stochastic process. A density-independent process will randomly explore all population sizes, because population size does not affect the growth rate. It is like a random walk on a flat surface. In contrast, a regulated process is like a random walk in a bowl; the population wanders about the bottom, but its random paths are ultimately bounded. Stochastic boundedness is a general property of density-dependent models, including the stochastic theta-logistic model (Diserud & Engen 2000) and its special cases the stochastic Gompertz (Dennis et al. 2006), theta-Ricker, and logistic models (Smitalova & Sujan 1992). Other biological processes, such as predator-prey interactions with global stability (Ives et al. 2003), can also lead

to this type of regulation where the process wanders stochastically around a confined region of population size.

An important observation about regulated stochastic population processes is that many can be recast as an Ornstein-Uhlenbeck (O-U) stochastic process (Ricciardi 1977; Turelli 1986). The O-U process (Karlin & Taylor 1981) is a diffusion process where the growth rate is a linear function of distance from some mean level:

$$dY_t = c(\overline{Y} - Y_t)dt + \sigma dW_t . \qquad [14]$$

Here Y is some function of the population size, for example log N, and $\overline{Y}$ is the mean to which the process reverts with a strength of reversion defined by the parameter c. Stochasticity is specified by the Weiner process W_t with a variance of σ. If Y_t is greater than $\overline{Y}$ the growth term is negative and Y declines, whereas if Y_t is less than $\overline{Y}$ the growth term is positive and Y increases. For this reason, the O-U is called a mean-reverting process. The O-U process has been extensively studied in the context of statistical physics and statistical economics (e.g., Dixit & Pindyck 1994), and those fields have provided many theoretical results. The distribution of $Y_{t+\tau}$-Y_t in the O-U process is normal, with a mean of $\overline{Y} + (Y_t - \overline{Y})e^{-c\tau}$ and a variance of $(\sigma^2 / 2c)(1 - e^{-2c\tau})$. The degree of correlation between $Y_{t+\tau}$ and Y_t falls off exponentially with τ. The asymptotic quasi-extinction times for O-U processes are exponentially distributed (Nobile *et al.* 1985; Larralde 2004; Alili *et al.* 2005). The close relationship between the O-U process and stochastic density-dependent population processes explains why extinction times are typically found to be exponentially distributed in stochastic density-dependent models (Ricciardi 1977; Turelli 1986; Goodman 1987; Middleton & Nisbet 1997).

O-U processes show two extreme behaviors. When the pull towards the mean is weak (c is small), the paths strongly resemble a density-independent random walk (Eq. 4 with $\mu = 0$); the

variance of $Y_{t+\tau}$ - Y_t is approximately linear with time, at least until τ is large. In this case, a SEG with $\mu = 0$ can approximate the quasi-extinction probabilities for moderate time horizons and thresholds. At the other extreme, when the pull towards the mean is strong (c is big), the process becomes tightly regulated about the mean value. This behavior, for τ not too small, can be approximated by the pure non-process error model (Eq. 12):

$$\begin{aligned} Y_t &= \overline{Y} + \varepsilon_{np,t} \\ Y_{t+\tau} &= \overline{Y} + \varepsilon_{np,t+\tau} \end{aligned} \qquad [15]$$

Here $\overline{Y}$ is the long-term mean population size, a.k.a. the carrying capacity. This approximation works because the correlation between Y_t and $Y_{t+\tau}$ falls off very rapidly for large c, so $Y_{t+\tau}$ is approximately normal with mean $\overline{Y}$ and variance $\sigma^2 / 2c$.

Recognizing these extreme behaviors in the O-U process suggests that a CSEG can also approximate the random mass properties of a stochastic regulated process for moderate forecast lengths. The CSEG is a combination of an SEG and a pure Gaussian error model, after all, and can thus be used to imitate both extremes.

To illustrate the CSEG approximation for density-dependent processes, we used a stochastic model with Ricker density dependence (Sabo et al. 2004):

$$\log N_{t+1} = \log N_t + r - |r| N_t / K + \varepsilon_t, \qquad [16]$$

where ε_t is a normally distributed variable with mean zero and variance σ_p^2, r is the intrinsic rate of increase, K is the carrying capacity, and N_t is the total population size. Two specific cases were examined: moderate density dependence (r = 0.02) and strong density dependence (r = 0.2). For both examples, K was set at 1000, σ_p^2 at 0.01, and N_0 was drawn randomly from the stochastic equilibrium.

Figures 6a and 6b show sample realizations of the simulations with moderate (right panels) and strong (left panels) density dependence. A plot of the variance in log $N_{t+\tau}/N_t$ as a function of τ for the model with moderate density dependence (panel c) shows that the variance will eventually plateau, but this does not occur within the 100 years of the simulation. For the model with strong density dependence, the variance quickly reaches a plateau (panel d). Panels e and f compare the CSEG's quasi-extinction probabilities to the actual probabilities observed in the stochastic Ricker simulations. These panels show that a CSEG can successfully approximate the two-dimensional quasi-extinction surface for these two density-dependent processes. Sabo and Gerber (2007) give other examples of CSEG approximations for populations regulated by predator-prey interactions, and we discuss another example using a regulated multi-species community in the following section.

Estimated versus theoretical stochastic approximations

The previous sections have discussed the random mass properties of several important classes of population processes, and illustrated the power of a simple stochastic model (the CSEG) to approximate their quasi-extinction probabilities. This completes step 1 of our statistical modeling outline (Figure 1c): we have used statistical theory to select a single approximating model that is valid for broad classes of possible generating processes. In addition because the CSEG was originally developed as a solution to the problem of measurement error in census data (Holmes 2001; Holmes & Fagan 2002; Lindley 2003; Holmes 2004; Staples *et al.* 2004), the CSEG approximation will simultaneously cope with non-process errors caused by measurement errors in the data collection step.

While the previous sections focused on the existence of a theoretical CSEG approximation, this section focuses on the estimation of the theoretical CSEG from population count data. This is the second step illustrated in Figure 1c: estimation of the random mass model. To illustrate the performance of estimated CSEGs, we make use of two different cross-validation studies, both of which focus on forecasting 80% population declines. The first study uses simulated data from three different cyclic population processes. These were chosen because they illustrate CSEG performance for processes with strong population feedbacks. These feedbacks generate high levels of non-process error. Other cross-validation studies have examined the performance of the CSEG approximation for non-cyclic processes (Holmes 2001; Morris & Doak 2003; Staples *et al.* 2004). The goal of our second cross-validation study is to test CSEG forecasts using a large dataset of actual time series from species of conservation concern.

Parameter estimation for the CSEG

The CSEG is an example of a state-space model with Gaussian errors, a class of models with well-developed estimation methods. One standard and flexible maximum-likelihood method for state-space models is the Kalman filter (Harvey 1989, section 3.4). Lindley (2003) and Holmes (2004) have shown how to apply the Kalman filter to the CSEG. Extended Kalman filters also exist which allow for non-Gaussian errors. The Kalman algorithm easily deals with missing values, and allows for the incorporation of supplementary data. Other parameter estimation approaches are also available. For example, restricted maximum likelihood (REML) can take advantage of the special correlations between counts in a CSEG (Staples et al. 2004). Standard statistical packages can be used for REML estimation (Dennis et al. 2006 show an

algorithm for the corrupted Gompertz of which the CSEG is a special case). Finally, a slope method has been developed (Holmes 2001) which performs a linear regression on the variance versus τ plots (such as in Figure 5b) to estimate the critical σ_p^2 term. Our experience is that the slope method is most robust when the data are generated from a strongly cyclic process, but this increased robustness comes at the cost of an increased bias. In the following cross-validations, we used the slope estimation method, because the Kalman filter and REML methods gave poor estimates for the strongly cyclic data produced by our examples. The Kalman filter in particular was often unable to separate σ_p^2 and σ_{np}^2 even with 20 to 30 years of our simulated cyclic data.

There is still much research to be done on robust estimation methods for CSEGs and their variants. In particular, further statistical research is needed to understand how to include any non-quantitative knowledge we might have about the population's life history, and how to adjust for multi-year correlations in the data generated by the population dynamics.

Simulation studies of CSEG forecasts for cyclic processes

We used a Monte Carlo approach to study the performance of our estimated CSEGs on large numbers of time series simulated from the same stochastic process. Using a particular stochastic model (hereafter referred to as the 'base' model), we randomly generated 1000 parameterization periods with lengths of 10, 20, or 30 years. To draw these randomly from the distribution of possible parameterization periods, we first allowed the simulation to run for 100 years. After this "burn-in" period, the data were collected for each parameterization period, $\{O_1, O_2, ..., O_k\}$. A CSEG was then estimated from each parameterization period using the slope method (Holmes 2001, 2004). In this manner, we obtain 1000 estimated CSEGs, which were used to forecast the probability of an 80% population decline within the next 50 years. To

determine the *actual* probability of 80% decline, we used the base model to simulate 1000 random 50-year trajectories forward from the end of the parameterization period. These simulations were started from the full population state (i.e. age-structure or multi-species densities depending on the model) at the end of each parameterization period. Thus, for each of the 1000 simulated periods, we obtain a CSEG estimate for the probability of quasi-extinction and an independent actual probability of quasi-extinction.

To calculate the quasi-extinction probabilities, however, we have to define the quasi-extinction threshold a little more explicitly. Specifically, to what population size is the 80% decline relative? In PVAs, some type of average of the last 3-5 censuses is often used, to avoid having estimates be adversely affected by the measurement error or other non-process error in the last census period, O_k. In this paper, we use $\hat{N}_k$, which is a maximum-likelihood estimate of the count at the end of the parameterization period with the non-process error removed. Figure 7 shows examples of $\hat{N}_t$ (the grey lines). $\hat{N}_k$ is a fourth parameter that must be estimated during CSEG estimation.

As discussed in the introduction, this paper is focused on using the CSEG to estimate a population process' expected quasi-extinction probability or the propensity of the process to experience quasi-extinction. Therefore, we cross-validate our CSEG estimates against the true expected probability of quasi-extinction:

$$\mathrm{E}[Pr(qe)] = \sum_{\{O_1,O_2,...,O_k\}} \Pr(\{O_1,O_2,...,O_k\})\, Pr(\text{80\% decline in 50 years} \mid \{O_1,O_2,...,O_k\}).$$

Here $\{O_1,O_2,...,O_k\}$ denotes a simulated parameterization period. $Pr(\text{80\% decline in 50 years} \mid \{O_1,O_2,...,O_k\})$ is the actual probability of 80% decline given that parameterization period, and

$\Pr(\{O_1, O_2, ..., O_k\})$ is the probability of the parameterization period. $\Pr(\{O_1, O_2, ..., O_k\})$ is 1/1000 since our parameterization periods are random samples from the stochastic equilibrium.

We perform simulations of three very different population models, all of which generate cycles: a stage-structured model (Figure 7a), a density-dependent model with over-compensating dynamics (Figure 7b), and a multi-species model with four interacting species (Figure 7c). For the stage-structured model, we used the Chinook salmon model (Eq. 8) and estimated the CSEGs from the spawner stage only. The chosen parameterization (given in Figure 5), when coupled with environmental stochasticity, produces strongly fluctuating spawner counts (Figures 5a and 7a). We next simulated an over-compensating, density-dependent process using the stochastic Ricker model (Eq. 16). The parameters chosen for this model ($K = N_0 = 1000$, $r = 0.02$, $\sigma_p^2 = 0.04$) are taken from recently published PVA analyses for density-dependent processes (McCarthy *et al.* 2003; Sabo *et al.* 2004). With these parameters, an interaction between the density dependence and the noise term leads to large oscillations in the population abundance. To generate the multi-species time series, we used a first-order, multivariate, autoregressive (MAR-1) process. In this model, the dynamics of each species is described by a discrete stochastic Gompertz model:

$$\log N_{i,t+1} = g + b \log N_{i,t} + \varepsilon_{i,t}, \qquad [17]$$

where g is the growth rate, b is the strength of the density dependence, and $\varepsilon_{i,t}$ is a normally distributed variable with mean zero and variance σ_i^2. Multi-species dynamics are modeled by extending Eq. 17 (Ives et al. 2003):

$$\mathbf{X}_{t+1} = \mathbf{G} + \mathbf{B}\mathbf{X}_t + \mathbf{E}_t. \qquad [18]$$

Here $\mathbf{X}_t$ is a vector of the population sizes for each species at time t, $\mathbf{G}$ is a vector of their growth rates, $\mathbf{B}$ is the community matrix describing the strength of self-regulation (diagonal elements)

and interspecies interactions (off-diagonals), and $\mathbf{E}_t$ is a process noise vector. We parameterized the MAR-1 process using estimates from a zooplankton community in Peter Lake, WI, USA (Ives et al. 2003). To estimate and forecast risks, we used the time series for only one species (large phytoplankton), ignoring the other species (small phytoplankton, daphnia, non-daphnia zooplankton). Fluctuations due to interactions with the other species create non-process variability in the large phytoplankton's trajectories.

Figure 8 shows CSEG estimates of the expected probability of decline, E[*Pr*(*qe*)], using 10-, 20-, and 30-year parameterization periods. The first thing to notice is that 10-year parameterization periods are insufficient for estimating quasi-extinction risks. Although the actual estimates are not terribly biased, the uncertainties on the estimates range from 0 to 1. Thus, for the rest of the discussion, we refer only to those results with 20- or 30-year parameterization periods. Using these longer parameterization periods, the mean estimated CSEG risks (black dots) are close to and show a similar overall shape as the actual risks (solid lines) but are not dead-on; they are biased up or down depending on the model. The estimated risks are biased because the slope method produces a biased estimate of σ_p^2. This bias can be approximately halved by estimating the bias with parametric bootstrapping (Wilcox 2004). Even though the CSEG estimates are biased, the close correspondence between estimated risks and actual risks is striking given that all three models produce strongly oscillatory data with high non-process variability.

The boxes and whiskers in Figure 8 show the precision of the estimates, enclosing 50% and 95% of the estimates respectively. The line in the middle of each box represents the median. The inner first quartiles (covering 50% of all estimates) are quite small for the MAR and salmon simulations. In addition, for these two population dynamics, the 95% ranges of the estimates

were less than [0,1] at both short (10-20 year) and long (30+ year) forecast lengths. For the Ricker model, although the short-term (10- and 20-year) forecasts have low variability (Figures 8e,f) the long-term forecasts have very wide 95% ranges. This occurs because the μ parameter (which measures trend) should have been constrained to zero for the Ricker model. Because this process reverts to the long-term mean population size very slowly, however, the μ estimates for each time series ranged widely between positive and negative values.

Estimating and forecasting are known to be difficult for processes with $\mu = 0$ (flat trend), because even small errors in estimating μ lead to large errors in the estimated long-term population size. This was less of a problem for the MAR example since that process fluctuates rapidly around the long-term mean. There has been recent research on estimating and forecasting extinction risks for density-dependent processes using a discrete Gompertz model with non-process error (Dennis et al. 2006), which may be a better way to approach estimation for slowly reverting processes, like our Ricker example. This model is essentially Eq. 17 observed with Gaussian error, so the CSEG is a special case of the discrete Gompertz model (albeit without mean reversion).

Studies on CSEG forecasts for real time series

Simulations are useful for studying population dynamics, but the models chosen for a simulation study are not necessarily representative of typical populations. For our second cross-validation study, we looked at the performance of CSEGs estimated from actual time series data. We assembled a database of 60 time series from populations being monitored for conservation or management reasons, obtained from literature searches and through direct contact with governmental agencies across the world (Appendix S1). All the time series are at least 30 years

long. The majority (40) come from populations that are at high risk and officially listed by a conservation agency at endangered or threatened levels (or the equivalent).

Our methods are similar to those of other cross-validations using real data (Brook *et al.* 2000; Holmes & Fagan 2002; Holmes *et al.* 2005), but add analyses to examine the precision, not just the bias, of estimates. Each time series was divided into a 20-year parameterization period followed by a 10-, 20-, or 30-year forecast period. The handful of much longer time series were segmented to provide a larger sample size; when a long time series was segmented, however, the parameterization periods were never allowed to overlap. For each time series a CSEG was estimated from the parameterization period using the slope method. The CSEG was used to make a prediction concerning whether the quasi-extinction threshold was reached during the forecast period (10-, 20- or 30-year depending on the analysis). Predicted risks were then compared to the actual numbers of quasi-extinctions in the forecast periods.

We examined the estimates in three different ways. In our first analysis, the actual number of quasi-extinctions in the entire database was compared to the expected number using the CSEG estimates at different thresholds. This assessed the systematic bias in the method (over- or under-estimation), and is analogous to the analysis of E[$Pr(qe)$] shown in Figure 8. The goal of this analysis is to quantify whether we can properly estimate the risk on average. In the second analysis, we ranked the time series by their CSEG estimated quasi-extinction probabilities and compared the actual and predicted cumulative number of quasi-extinctions in the sorted dataset. This quantifies the degree to which we can properly estimate the risk for a specific population (rather than the average risk across populations). Thus, we ask whether a low estimated risk for a specific population corresponds to a low actual risk. In the third analysis, the 95% and 50% confidence intervals of the CSEG estimates were estimated using

parametric bootstrapping. This analysis informs us about the precision of the estimated quasi-extinction probabilities.

Figure 9 shows the estimated (dots) and actual (solid line) proportion of quasi-extinctions in the entire database within 10-, 20-, and 30-year forecast periods following a 20-year parameterization period. The observed and predicted frequencies match well for all forecasts. This indicates that the overall bias of the CSEG forecasts is low, provided 20 years of data were used for parameterization.

Figures 10a, 10b, and 10c show the cumulative number of 80%, 50% and 20% declines respectively over a 10-year forecast period and a 20-year parameterization period. The dotted line is the cumulative number of quasi-extinctions predicted by the CSEGs, and the black line is the actual number observed in the sample. If there were no correlation between the expected number and actual number, the black line would be straight. Instead the black line is convex, which shows that the estimated risks are correlated with the actual risks; a low estimated risk is generally associated with a low actual risk. However, the actual line is more concave than expected. This means that we tend to *underestimate* low to moderate risks. This is the same pattern seen in the salmon models (Figure 8b,c) which suggests that this bias may be due to a biased estimate of σ_p^2. Due to the limited number of time series lasting longer than 30 years, we could not effectively test the cumulative distributions for forecasts longer than 10 years.

Figure 10 shows the estimated 95% CIs (grey lines) and 50% CIs (black lines) for the CSEG-estimated quasi-extinction probabilities. Panels 10d, 10e, and 10f show results for 80%, 50% and 20% declines respectively, over a 10-year projection period. The 50% CIs are quite narrow, while the 95% CIs are wide but still less than [0,1]. The precision is better for estimates of the more severe 80% and 50% declines. A similar result was seen by Sabo et al. (2004).

Discussion

Random mass properties are the ensemble patterns that emerge from a large collection of samples from a stochastic process. In this paper, we have drawn a distinction between statistical models, which seek to capture the random mass properties of stochastic population processes, and mechanistic models, which seek to portray the biological processes responsible for observed population dynamics. We have sought to show how statistical models of a particular random mass property, the risk of quasi-extinction, can be inferred from time series data by drawing on existing theoretical work on stochastic processes. We showed that simple statistical models can accurately approximate the quasi-extinction risk across different forecast lengths and risk thresholds, for a variety of different population processes. We have focused on a particular statistical model, the corrupted stochastic exponential Gaussian model (CSEG), and have shown that this three-parameter model can be adequately estimated from 20-30 years of data. Using two cross-validations, one based on simulations of cyclic populations and the other based on a large dataset of time series from species of concern to conservation, we illustrated that the CSEG can be used to estimate quasi-extinction risk with a relatively low bias and a 95% CI generally much smaller than [0,1].

Arguing that the CSEG is the panacea for all quasi-extinction estimation is not the point of this paper, however. There is ongoing theoretical work on the subject of stochastic approximations for population processes, and there remains much to learn especially about the random mass properties of density-dependent processes. It would be myopic to assert that the CSEG is the be-all and end-all, despite its prowess at modeling quasi-extinction for important classes of population dynamics. Rather, the point of this paper is to illustrate and advocate for

statistical models derived from theoretical research concerning the random mass properties of population trajectories. The main strengths of this approach are threefold. First, if a convergent approximation can be found that works for several broad classes of dynamics, one need not know the underlying mechanistic population process to correctly forecast quasi-extinction. This is important because there is often too little data to estimate the underlying mechanisms. Second, a statistical model with few parameters requires much less data for estimation, and is much less likely to be compromised by over-fitting. Finally, the parameters of a statistical model can be estimated and their uncertainty quantified using standard statistical techniques. Our inability to rigorously quantify the uncertainly of our predictions from parameter-rich, mechanistic models is a serious problem, and one too rarely acknowledged.

Confronting the criticisms of quantitative PVA

Although we argue for a statistical approach to PVA, our models are still open to many of the criticisms that have been leveled at PVA models in general. Specifically, PVA models are often criticized for their simplicity and lack of precision (Taylor 1995; Ludwig 1996; Beissinger & Westphal 1998; Ludwig 1999; Fieberg & Ellner 2000; Coulson *et al.* 2001; Ellner *et al.* 2002). Their critics contend that because PVA models fail to address the correct causes of population dynamics, they must yield biased and/or imprecise estimates of the consequences of these causes (i.e., the population dynamics). These criticisms also assert that PVA predictions are unreliable because 1) the data used to estimate model parameters are marred by systematic or random observer errors, 2) the PVA model ignores too many important processes in the population dynamics, and 3) sparse datasets lead to highly uncertain parameter estimates and wide

confidence intervals on the estimated risk. Here we revisit these criticisms in light of our results regarding statistical PVA models.

First, in fairness to previous critiques of PVA, we note that conservation biologists are indeed faced with data riddled with observation errors. Observer errors can certainly corrupt and bias estimates of the true yearly variations experienced by a population. Random observation errors present the biggest problems for those species with moderate growth rates and process errors. In these situations, extinction risk estimates are highly uncertain even with error-free data (Meir & Fagan 2000). CSEG models provide an explicit way of addressing many of these problems, and greatly reduce the effects of observation errors on the quasi-extinction risk forecast (Holmes 2001; Lindley 2003; Holmes 2004; Staples *et al.* 2004). This research shows that the bias due to observation error can be quantified and its effects mitigated using a state-space model, like the CSEG.

A second common criticism of PVA models -- and one of the central issues addressed in this paper -- is that most PVA models are just too simple to be believable. Critics correctly point out that most PVAs ignore many biological complexities. There are many examples of the problems with PVA models that are missing age or stage structure (Fieberg & Ellner 2000; Ellner *et al.* 2002; Wilcox & Possingham 2002), individual variations (Fox & Kendall 2002), demographic stochasticity (Lande 1993; Engen *et al.* 2003; Engen *et al.* 2005), density dependence (Foley 1994; Sabo *et al.* 2004), and species interactions (Gerber *et al.* 2005; Sabo & Gerber 2007). For a population whose quasi-extinction risks need to be estimated, however, the available data will often be too limited to specify these details with confidence. For example, there are serious difficulties in determining even basic details like density dependence with confidence (Dennis & Taper 1994). We argue that the best solution to the problem of

unknowable details is the development of statistical models based on convergent statistical patterns. We have shown several examples of how complex details can average out when we look at ensemble properties, and how these ensemble properties can have similar patterns across different types of population dynamics – even cyclic dynamics.

Finally, there is what is known as the [0,1] criticism. This is the claim that sparse data and strong environmental variations, when coupled, lead to quasi-extinction risk estimates whose confidence intervals span the entire range of probabilities (Ludwig, 1996; Fieberg and Ellner, 2000; Ellner et al., 2002). We have alluded to this criticism throughout the paper in our discussion of the CSEG predictions, which often span a much smaller range. Along similar lines, some researchers have found that risk estimates using simple PVA models are reasonably precise only for forecasts that are much shorter (e.g., 20%) than the number of years available for parameterization (Fieberg and Ellner, 2000).

We do agree with this criticism when too little data (i.e., only 10 years) are used for parameterization. As we have seen in the simulations of this study and other cross-validations (Holmes 2004), a ten-year time series is too short for estimating quasi-extinction. But our conclusions are much more optimistic when a 20-year time series is available. In this case, relatively unbiased and precise quasi-extinction estimates could be made for up to two and a half times the length of the parameterization period for our declining and rapidly fluctuating populations (but not the slowly fluctuating populations). This agrees with our results from our other simulation and cross-validation studies (Holmes 2001; Holmes & Fagan 2002; Holmes 2004; Sabo & Gerber 2007). With real data from species of conservation concern, we were only able to fully cross-validate for 10-year forecasts given data limitations, but here again found low average bias, correlation between estimated and real risks, and confidence intervals that were

much less than [0,1]. Although we argue that with 20-year of data the [0,1] problem is not as severe or ubiquitous as critics assert, we certainly agree that quasi-extinction estimates can have high uncertainty -- even with 20+ years of data. Here the real advantage of a statistical approach emerges. With a theoretically derived statistical model, the uncertainty in the quasi-extinction estimates can be established via theory and can be estimated using traditional statistical methods.

Conclusion

We do not dispute the importance of mechanistic models for testing hypotheses about underlying mechanisms or for simulating the effects of specific management actions. If the only goal is to forecast quasi-extinction, however, then we argue for a statistical model based on a small set of estimable parameters. Appropriate statistical models can be derived from the theory of stochastic population processes, and they yield a risk metrics whose uncertainty can be estimated from the type of data most common for species of concern – time series of population counts. It is true that in some cases these estimates will have high variance, but we argue that statistical models both reduce this variance and allow us to quantify the uncertainty in more a traditional manner. In contrast, for all but the most well-studied species any mechanistic population model will be replete with poorly estimated parameters. In such cases, meaningful uncertainty estimates are impossible. Critics of PVA tend to argue that the devil is in the details. We counter that the compulsive urge to account for intricate biological details ignores the fact that these details average out thanks to the stochastic and multiplicative nature of population growth. If we focus only on the details, we lose sight of the common patterns that govern the ensemble behavior of population trajectories.

Acknowledgements

SV was supported by a fellowship from the National Research Council. WFF was supported by Dept. of Defense – SERDP contract SI-1475. We thank the National Center for Ecological Analysis and Synthesis for their logistic support during the inception of this project.

References

Alili L., Patie P. & Pedersen J.L. (2005) Representations of the first hitting time density of an Ornstein-Uhlenbeck process. *Stochastic Models*, 21, 967-980.

Beissinger S.R. & McCullough D.R. (2002) *Population viability analysis*. University of Chicago Press, Chicago.

Beissinger S.R. & Westphal M.I. (1998) On the use of demographic models of population viability in endangered species management. *Journal of Wildlife Management*, 62, 821-841.

Boyce M.S. (1992) Population viability analysis. *Annual Review of Ecology and Systematics*, 23, 481-506.

Brook B.W., O'Grady J.J., Chapman A.P., Burgman M.A., Akçakaya H.R. & Frankham R. (2000) Predictive accuracy of population viability analysis in conservation biology. *Nature*, 404, 385-387.

Caswell H. (2000) *Matrix population models: construction, analysis, and interpretation*. Sinauer, Sunderland, MA, USA.

Coulson T., Mace G.M., Hudson E. & Possingham H. (2001) The use and abuse of population viability analysis. *Trends in Ecology & Evolution*, 16, 219-221.

DeMaster D., Angliss R., Cochrane J., Mace P., Merrick R., Miller M., Rumsey S., Taylor B., Thompson G. & Waples R. (2004) Recommendations to NOAA Fisheries: ESA listing criteria by the Quantitative Working Group 10 June 2004. U.S. Department of Commerce, NOAA Tech. Memo. NMFSF/SPO-67, 85pp.

Dennis B., Munholland P.L. & Scott J.M. (1991) Estimation of growth and extinction parameters for endangered species. *Ecological Monographs*, 61, 115-143.

Dennis B., Ponciano J.M., Lele S.R., Taper M.L. & Staples D.F. (2006) Estimating density dependence, process noise, and observation error. *Ecological Monographs*, 76, 323-341.

Dennis B. & Taper M.L. (1994) Density dependence in time series observations of natural populations: estimation and testing *Ecological Monographs*, 64, 205-224.

Diserud O.H. & Engen S. (2000) A general and dynamic species abundance model, embracing the lognormal and the gamma models. *The American Naturalist*, 155, 498-511.

Dixit v.K. & Pindyck R.S. (1994) *Investment under uncertainty*. Princeton University Press, Princeton, NJ.

Ellner S.P., Fieberg J., Ludwig D. & Wilcox C. (2002) Precision of population viability analysis. *Conservation Biology*, 16, 258-261.

Engen S., Lande R. & Saether B.E. (2003) Demographic stochasticity and allee effects in populations' with two sexes. *Ecology*, 84, 2378-2386.

Engen S., Lande R., Saether B.E. & Weimerskirch H. (2005) Extinction in relation to demographic and environmental stochasticity in age-structured models. *Mathematical Biosciences*, 195, 210-227.

Fagan W.F. & Holmes E.E. (2006) Quantifying the extinction vortex. *Ecology Letters*, 9, 51-60.

Feller W. (1968) *An introduction to probability theory and its applications*. Wiley, New York, NY, USA.

Fieberg J. & Ellner S.P. (2000) When is it meaningful to estimate an extinction probability? *Ecology*, 81, 2040-2047.

Foley P. (1994) Predicting extinction times from environmental stochasticity and carrying capacity. *Conservation Biology*, 8, 124-137.

Fox G.A. & Kendall B.E. (2002) Demographic stochasticity and the variance reduction effect. *Ecology*, 83, 1928-1934.

Furstenberg H. & Kesten H. (1960) Products of random matrices. *Annals of Mathematical Statistics*, 31, 457-469.

Gerber L.R., McCallum H., Lafferty K.D., Sabo J.L. & Dobson A. (2005) Exposing extinction risk analysis to pathogens: Is disease just another form of density dependence? *Ecological Applications*, 15, 1402-1414.

Goodman D. (1987) The demography of chance extinction. In: *Viable Populations for Conservation* (ed. Soule M). Cambridge University Press, Cambridge, UK, pp. 11-34.

Harvey A.C. (1989) *Forecasting, structural time series models and the Kalman filter*. Cambridge University Press, Cambridge, UK.

Holmes E.E. (2001) Estimating risks in declining populations with poor data. *Proceedings of the National Academy of Sciences of the United States of America*, 98, 5072-5077.

Holmes E.E. (2004) Beyond theory to application and evaluation: diffusion approximations for population viability analysis. *Ecological Applications*, 14, 1272-1293.

Holmes E.E. & Fagan W.E. (2002) Validating population viability analysis for corrupted data sets. *Ecology*, 83, 2379-2386.

Holmes E.E., Fagan W.F., Rango J.J., Folarin A., J.A. S., Lippe J.E. & McIntyre N.E. (2005) Cross validation of quasi-extinction risks from real time series: An examination of diffusion approximation methods. U.S. Department of Commerce, NOAA Tech. Memo. NMFS-NWFSC-67, 37pp.

Holmes E.E. & Semmens B. (2004) Population viability analysis for metapopulations: a diffusion approximation approach. In: *Ecology, Genetics, and Evolution of Metapopulations* (eds. Hanski I & Gaggiotti OE). Elsevier Press, pp. 565-598.

Ives A.R., Dennis B., Cottingham K.L. & Carpenter S.R. (2003) Estimating community stability and ecological interactions from time-series data. *Ecological Monographs*, 73, 301–330.

Karlin S. & Taylor H.M. (1981) *A second course in stochastic processes*. Academic Press, San Diego.

Lande R. (1993) Risks of population extinction from demographic and environmental stochasticity and random catastrophes. *American Naturalist*, 142, 911-927.

Lande R., Engen S. & Saether B. (2003) *Stochastic population dynamics in ecology and conservation*. Oxford University Press, Oxford.

Lande R. & Orzack S.H. (1988) Extinction dynamics of age-structured populations in a fluctuating environment. *Proceedings of the National Academy of Science USA*, 85, 7418-7421.

Larralde H. (2004) A first passage time distribution for a discrete version of the Ornstein-Uhlenbeck process. *Journal of Physics A: Mathematical and General*, 37, 3759-3767.

Lewontin R.C. & Cohen D. (1969) On population growth in a randomly varying environment. *Proceedings of the National Academy of Science USA*, 62, 1056–1060.

Lindley S.T. (2003) Estimation of population growth and extinction parameters from noisy data. *Ecological Applications*, 13, 806-813.

Ludwig D. (1996) Uncertainty and the assessment of extinction probabilities. *Ecological Applications*, 6, 1067-1076.

Ludwig D. (1999) Is it meaningful to estimate a probability of extinction? *Ecology*, 80, 298-310.

Mace G.M. & Lande R. (1991) Assessing extinction threats: toward a reevaluation of IUCN threatened species categories. *Conservation Biology*, 5, 148–157.

McCarthy M.A., Andelman S.J. & Possingham H.P. (2003) Reliability of relative predictions in population viability analysis. *Conservation Biology*, 17, 982-989.

Meir E. & Fagan W.F. (2000) Will observation error and biases ruin the use of simple extinction models? *Conservation Biology*, 14, 148-154.

Middleton D.A.J. & Nisbet R.M. (1997) Population persistence time: estimates, models, and mechanisms. *Ecological Applications*, 7, 107–117.

Morris W.F., Bloch P.L., Hudgens B.R., Moyle L.C. & Stinchcombe J.R. (2002) The use of population viability analysis in endangered species recovery planning: Past trends and recommendations for future improvement. *Ecological Applications*, 12, 708-712.

Morris W.F. & Doak D.F. (2003) *Quantitative conservation biology: theory and practice of population viability analysis*. Sinauer Associates, Sunderland, MA USA.

Nobile A.G., Ricciardi L.M. & Sacerdote L. (1985) Exponential trends of Ornstein-Uhlenbeck first-passage-time densities. *Journal of Applied Probability*, 22, 360–369.

Polya G. (1968) *Mathematics and Plausible Reasoning, Vol II*. Princeton University Press, Princeton, NJ.

Ricciardi L.M. (1977) *Diffusion processes and related topics in biology*. Springer-Verlag, New York.

Sabo J.L. & Gerber L.R. (2007) Single species PVA models are sometimes biased by species interactions. *Ecological Applications*, in press

Sabo J.L., Holmes E.E. & Kareiva P. (2004) Efficacy of simple viability models in ecological risk assessment: does density dependence matter? *Ecology*, 85, 328-341.

Smitalova K. & Sujan S. (1992) *A mathematical treatment of dynamical models in biological science*. Ellis Horwood Ltd, New York, NY, USA.

Staples D.F., Taper M.L. & Dennis B. (2004) Estimating population trend and process variation for PVA in the presence of sampling error. *Ecology*, 85, 923-929.

Taylor B.L. (1995) The reliability of using population viability analysis for risk classification of species. *Conservation Biology*, 9, 551-558.

Tuljapurkar S.D. (1989) An uncertain life: demography in random environments. *Theoretical Population Biology*, 35, 227-294.

Tuljapurkar S.D. & Orzack S.H. (1980) Population dynamics in variable environments. I. Long-run growth rates and extinction. *Theoretical Population Biology*, 18, 314-342.

Turelli M. (1986) Stochastic community theory: a partially guided tour. *Biomathematics*, 17, 321-339.

Wilcox C. & Possingham H. (2002) Do life history traits affect the accuracy of diffusion approximations for mean time to extinction? *Ecological Applications*, 12, 1163-1179.

Wilcox R.R. (2004) *Introduction to robust estimation and hypothesis testing*. 2nd edn. Academic Press, Burlington, MA.

Figure Legends

Figure 1. Reasoning using statistical and mechanistic modeling. a) In a mechanistic paradigm, the model is meant to mimic the data observed. The data are thus used to choose the model via some formal or ad hoc selection method. Once a model is selected its parameters are estimated, often from the same data. b) A familiar example of statistical reasoning is inference concerning a large sample mean. The Central Limit Theorem (CLT) for independent random variables says that the means of large samples converge to the normal distribution. Thus, in this case a theory concerning the random mass properties of samples is used to specify the model. Although the large-sample distribution is known, its parameters μ and σ^2 must be estimated from a small finite sample. The CLT also specifies the relationship between small samples and the distribution of large-sample means. c) The basic steps of building a statistical model based on the random mass properties of population trajectories: 1) a theory of the common stochastic patterns and model that emerge from diverse processes, 2) estimation of the theoretical stochastic model from the data, and 3) forecasting using the estimated model.

Figure 2. The statistical properties of pure random walks. a) Trajectories of a random walk, showing the fraction that decline below some threshold. b) The 2D quasi-extinction surface as a function of the forecast length (x-axis) and threshold (y-axis), shown here as a percentage decline from the population size at year 1. c) The quasi-extinction probability is shown as a function of the forecast length. d) The quasi-extinction probability is shown as a function of the threshold. e) The long-term distribution of log N is normal. f) The variance and mean of $\log N_{t+\tau} / N_t$ scale linearly with time.

Figure 3. Example of an SEG model used to approximate the quasi-extinction risk for total population counts in Chinook salmon. a) Multiple realizations of the total population trajectory from the salmon model. b) Variance and mean of log $N_{t+\tau}/N_t$ as a function of τ, showing the linear scaling of these parameters. c) A histogram of log N_{10}/N_1, showing a bell-shaped distribution (the right-hand tails are heavy). d) A histogram of log N_{50}/N_1, showing a better approximation to the normal distribution; the tails are no longer noticeably heavy. e) Actual probabilities of hitting 20%, 75%, and 90% decline (solid lines) versus those predicted from the appropriate SEG (dotted lines) as a function of forecast length. f) The same as in (e), but as a function of threshold value for three different forecast lengths. The parameter values for the salmon matrix (Eq. 7): $p = 0.4815$; $s_1 = 0.018$; $s_2 = 0.044$; $s_o = 0.8$; $b_3 = 0$; $b_4 = 0.216$; $b_5 = 1$; $m = 2747$; $\varepsilon_{i,t} \sim \exp(Normal(0, \sigma_i^2))$ with $\sigma_0^2 = 0.02$, $\sigma_1^2 = 0.13$, $\sigma_2^2 = 0.08$. The correlation coefficient between ε_1 and ε_2 was R = 0.2, and the correlation between ε_0 values for all age classes was R = 0.8. The latter represents ocean survival.

Figure 4. Example of an SEG model used to approximate the quasi-extinction risk in a stochastic metapopulation model. a) Multiple realizations of the total metapopulation trajectory from the simulations. b) Diagram of the basic metapopulation properties in this example. Each site disperses a different fraction of its population each year (the relative dispersal rates are shown by the size of the arrows). 80% of dispersers go to neighbors to the east and south, and 20% are distributed equally among all other sites in the metapopulation. Sites vary in their intrinsic population growth rates, but all are declining. Growth rates range from 0.99 to 0.80. Yearly growth rates vary (s.d. = 0.1) and are correlated between sites (R = 0.9). d) Actual

probabilities of hitting 20%, 75%, and 90% declines (solid lines) versus those predicted from the appropriate SEG (dotted lines) as a function of forecast length. f) The same as in (e), but as a function of threshold value for three different forecast lengths.

Figure 5. Example of a CSEG approximation to the quasi-extinction risk for spawner counts from the Chinook salmon model. a) Multiple realizations of the (logarithmic) spawner count trajectory. b) A plot of the variance in log $N_{5,t+\tau}/N_{5,1}$ as a function of τ. The transient behavior is evident for $\tau < 20$, but approaches linearity for larger τ. The intercept is non-zero. c) A histogram of log $N_{5,10}/N_{5,1}$, showing a bell-shaped distribution with slightly heavy tails. d) A histogram of log $N_{5,50}/N_{5,1}$, showing that the distribution is now more normal. e) Actual probabilities of hitting 20%, 75%, and 90% declines (solid lines) versus those predicted from the appropriate CSEG (dotted lines) as a function of forecast length. f) The same as in (e) but as a function of threshold for three different forecast lengths. Parameter values for the salmon matrix (Eq. 7): $p = 0.4815$; $s_1 = 0.018$; $s_2 = 0.044$; $s_o = 0.8$; $b_3 = 0$; $b_4 = 0.216$; $b_5 = 1$; $m = 2747$; $\varepsilon_{i,t} \sim \exp(normal(0, \sigma_i^2))$ with $\sigma_0^2 = 0.02$, $\sigma_1^2 = 0.13$, $\sigma_2^2 = 0.08$. The correlation coefficient between ε_1 and ε_2 was R = 0.2, and the correlation between ε_0 values for all age classes was R = 0.8. The latter is higher because it represents ocean survival that is highly correlated across age classes.

Figure 6. Example of CSEG approximations to the quasi-extinction risk for stochastic Ricker simulations with weak and strong density dependence. (a,b) Multiple realizations of each process. (c,d) The actual variance as a function of τ (solid line) and the CSEG approximation (dotted line). (e,f) Actual and CSEG quasi-extinction probabilities versus forecast length for

three different thresholds. (g,h) Actual and CSEG quasi-extinction probabilities versus threshold for three different forecast lengths. The CSEG parameters are (left panels) $\mu = 0,\ \sigma_p^2 = 0.005,$ $\sigma_{np}^2 = 0.01$; (right panels) $\mu = 0,\ \sigma_p^2 = 0.0005,\ \sigma_{np}^2 = 0.0158.$

Figure 7. Time series produced from the three simulated models used in cross-validation. a) A model for Chinook salmon. The data used for estimation and prediction are spawner counts (black line). b) A stochastic Ricker model. The data used are the total population counts (black line). c) A four-species predator-prey model. The data used for estimation and prediction are the counts for one species only (black line); the other species are ignored. The black lines include both process and non-process error. The grey lines show the maximum-likelihood estimated trajectory with process errors only (i.e., *N* in the CSEG equation). This is calculated from the CSEG model, which was estimated from the observed data (black lines). In the cross-validation of these simulations, the threshold was set relative to the estimated value of *N* (grey line) at the end of the parameterization period.

Figure 8. Cross-validation using simulations of the expected quasi-extinction probability as a function of forecast length (x-axes). The three rows refer to a Chinook salmon simulation (top panels), a stochastic Ricker model (middle panels), and a 4-species stochastic community (bottom panels). The solid lines show the actual mean probability of 80% decline observed in the simulations. The boxes and whiskers show the range of CSEG estimates obtained using a 10-year (left panels), 20-year (middle panels), and 30-year (right panels) parameterization period. The boxes enclose 50% of the CSEG estimates, and the whiskers show the range

containing 95% of the estimates. The black dots show the mean CSEG estimate. The CSEG parameters were estimated using the slope method.

Figure 9. Cross-validation using real time series data: the expected fraction of quasi-extinction within the dataset versus the actual fraction for 10-, 20- and 30-year forecasts. The sample size (number of time series) is different in each panel because there are fewer long time series in the dataset. The 95% CI error bars on the CSEG estimates were calculated using a binomial error model. A 20-year parameterization period was used for all time series, with the CSEG estimated via the slope method.

Figure 10. Cross-validation using real time series data: cumulative quasi-extinction probabilities in the long-term dataset. The left-hand panels show the observed and expected cumulative number of quasi-extinctions in a 10-year forecast, based on a 20-year parameterization period. The time series (x-axis) are ordered according to their CSEG-estimated quasi-extinction risk. The panels show a) the 80% decline threshold, b) the 50% decline threshold, and c) the 20% decline threshold. The right-hand panels show the 95% and 50% confidence intervals on the estimated probabilities for 80%, 50%, and 20% declines (panels d, e, and f respectively). Confidence intervals were calculated using parametric bootstrapping. The estimated CSEG was used to generate 1000 random 20-year parameterization periods. From each of these another CSEG was estimated to give 1000 bootstrapped CSEGs. The bootstrapped CSEGs were then used to generate quasi-extinction forecasts. The CIs thus show the variability of the bootstrapped quasi-extinction risks.

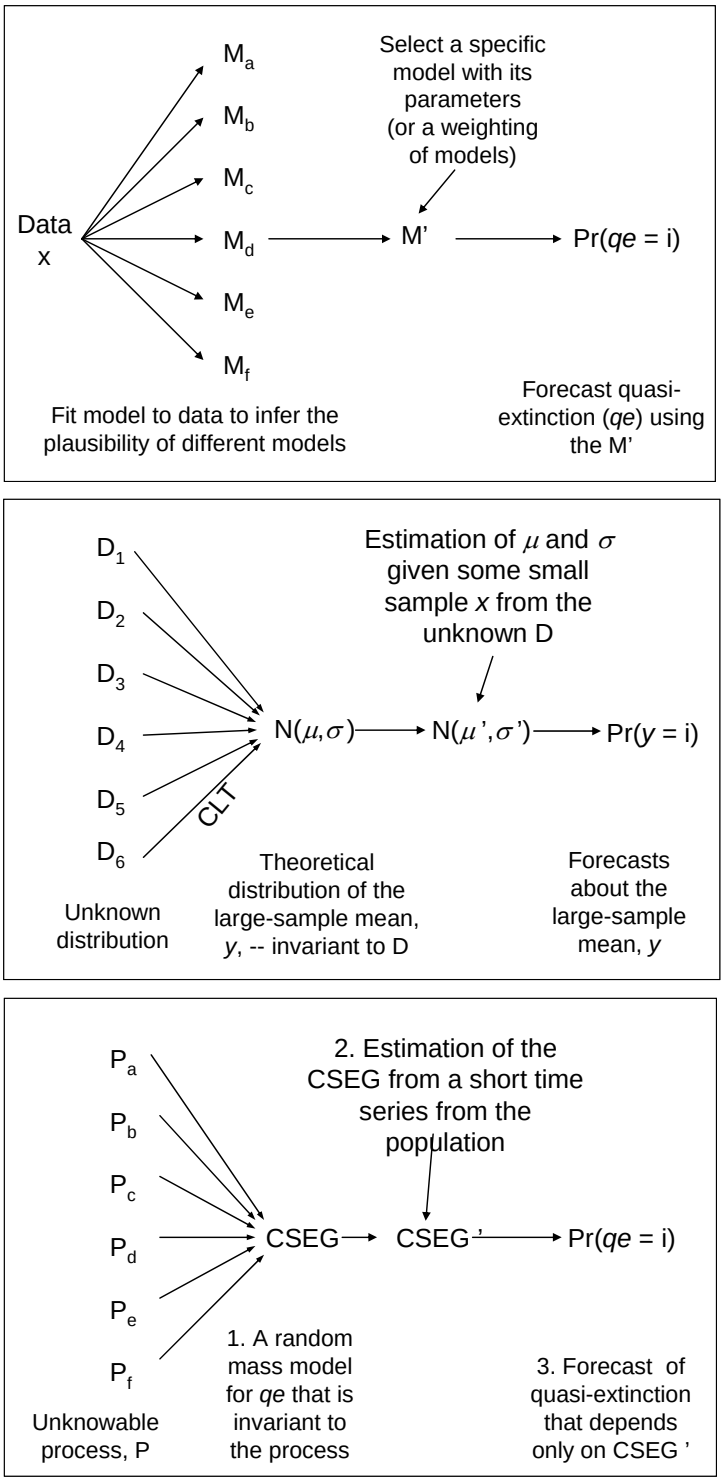
a
Select a specific model with its parameters (or a weighting of models)
Data x
M_a
M_b
M_c
M_d
M_e
M_f
M'
Pr(*qe* = i)
Fit model to data to infer the plausibility of different models
Forecast quasi-extinction (*qe*) using the M'
b
Estimation of μ and σ given some small sample *x* from the unknown D
D_1
D_2
D_3
D_4
D_5
D_6
CLT
$N(\mu,\sigma)$
$N(\mu',\sigma')$
Pr(*y* = i)
Unknown distribution
Theoretical distribution of the large-sample mean, *y*, -- invariant to D
Forecasts about the large-sample mean, *y*
c
2. Estimation of the CSEG from a short time series from the population
P_a
P_b
P_c
P_d
P_e
P_f
CSEG
CSEG'
Pr(*qe* = i)
Unknowable process, P
1. A random mass model for *qe* that is invariant to the process
3. Forecast of quasi-extinction that depends only on CSEG '

Fig. 2

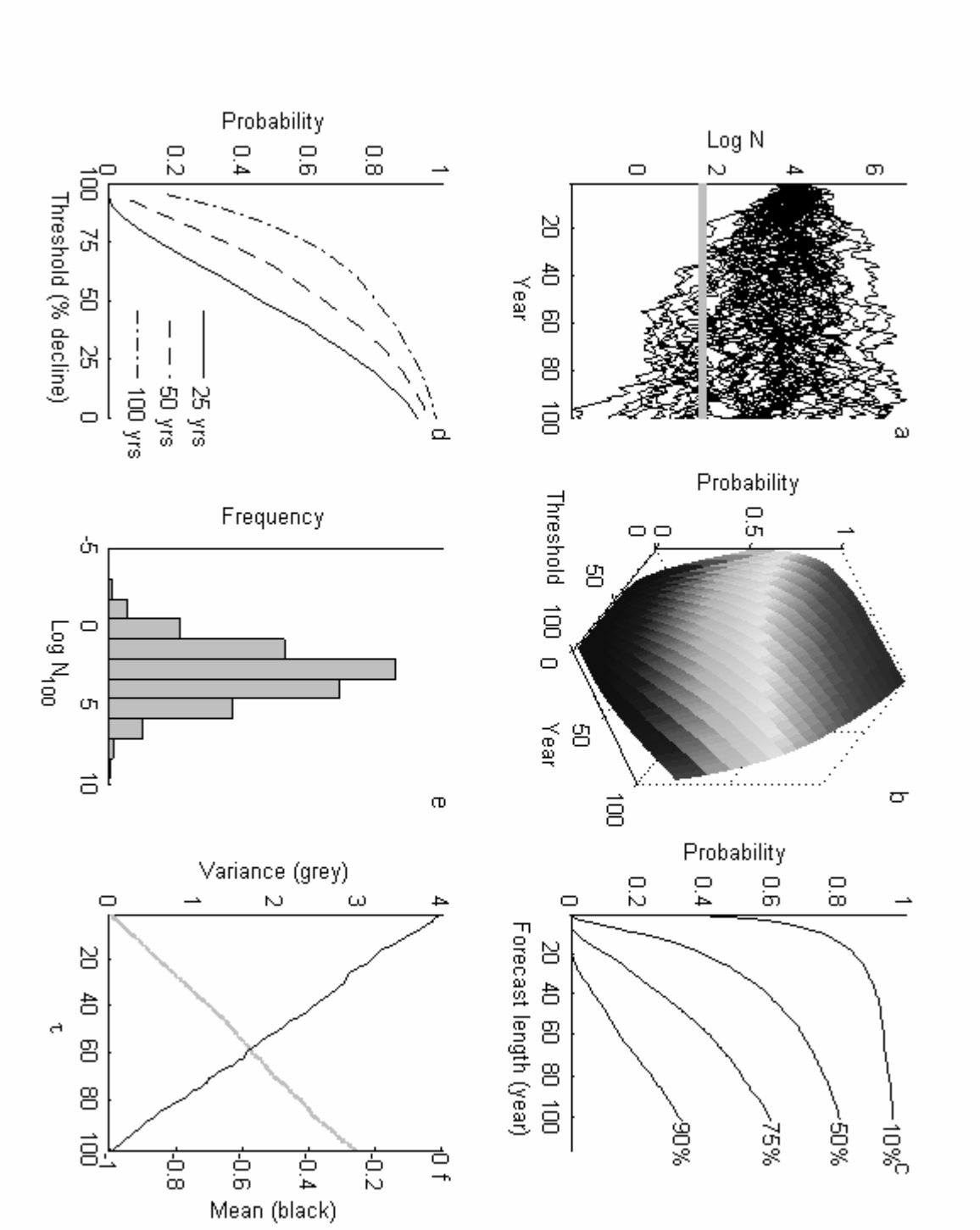
Log N
Year
a
Probability
Threshold
Year
b
Probability
Forecast length (year)
10%
50%
75%
90%
c
Probability
Threshold (% decline)
25 yrs
50 yrs
100 yrs
d
Frequency
Log N100
e
Variance (grey)
Mean (black)
τ
f

Fig. 3

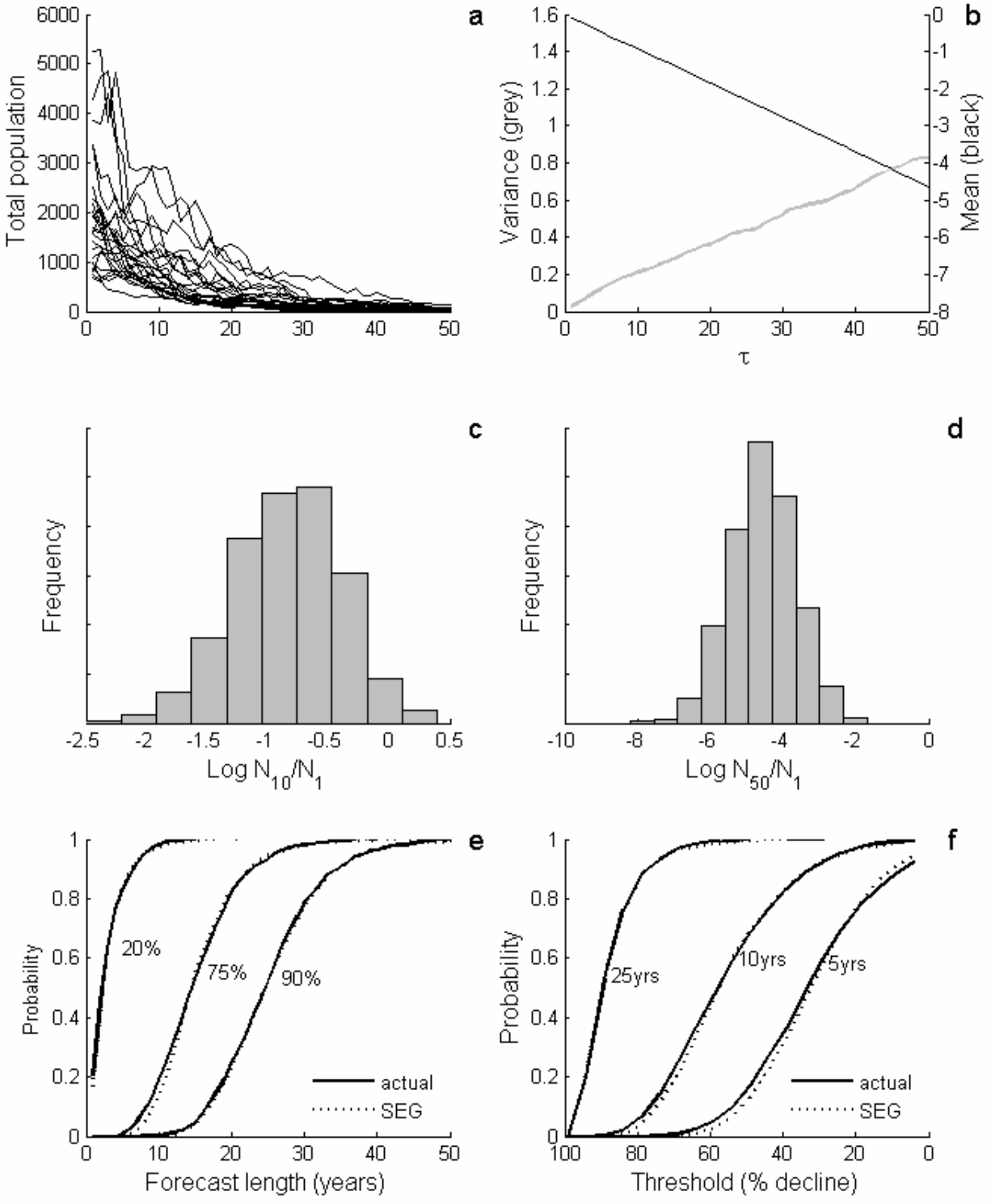
a
Total population
b
Variance (grey)
Mean (black)
τ
c
Frequency
Log N10/N1
d
Frequency
Log N50/N1
e
Probability
20%
75%
90%
actual
SEG
Forecast length (years)
f
Probability
25yrs
10yrs
5yrs
actual
SEG
Threshold (% decline)

Fig. 4

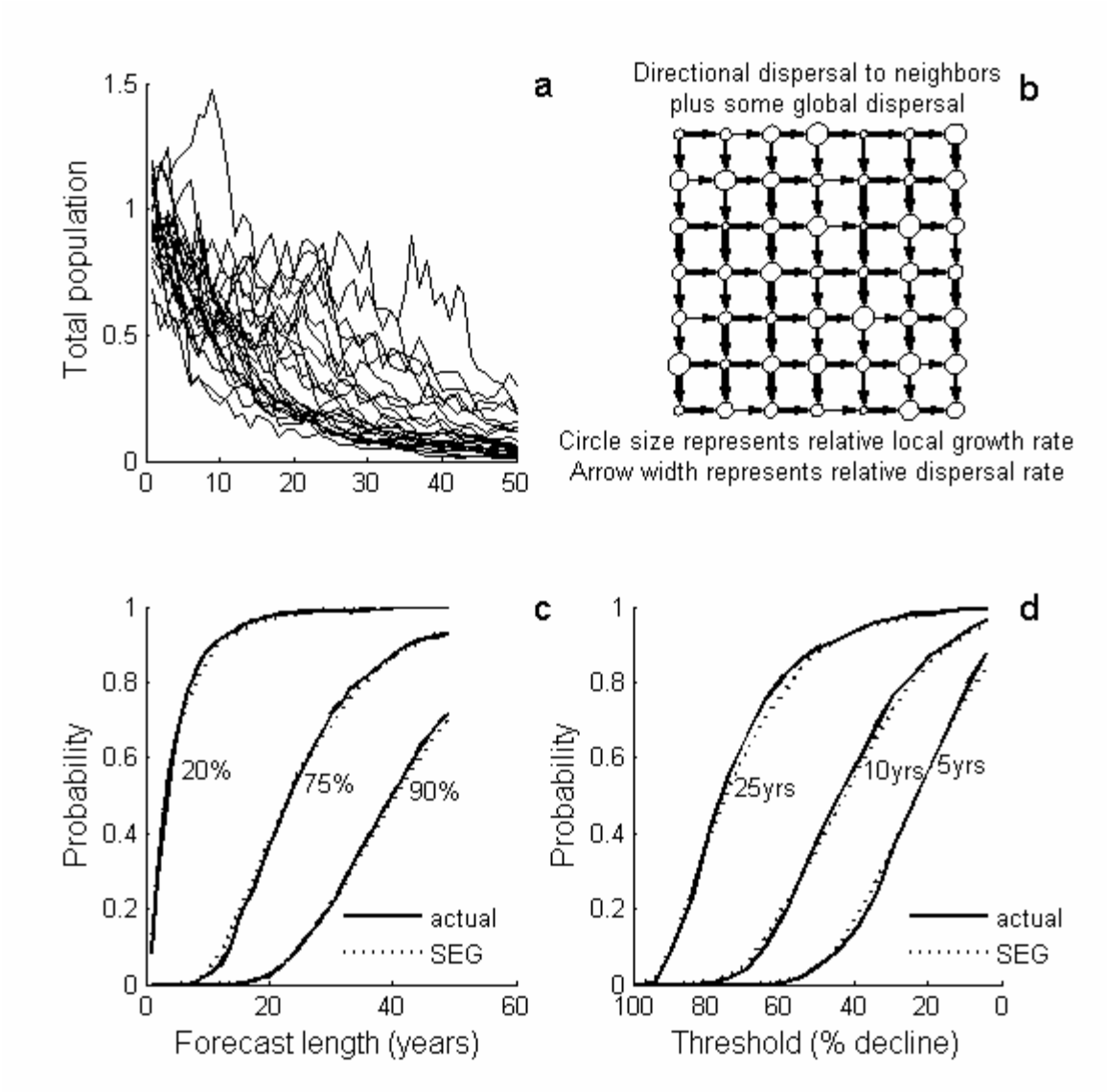
a
Total population
1.5
1
0.5
0
0
10
20
30
40
50
b
Directional dispersal to neighbors
plus some global dispersal
Circle size represents relative local growth rate
Arrow width represents relative dispersal rate
c
Probability
1
0.8
0.6
0.4
0.2
0
20%
75%
90%
actual
SEG
0
20
40
60
Forecast length (years)
d
Probability
25yrs
10yrs
5yrs
actual
SEG
100
80
60
40
20
0
Threshold (% decline)

Fig. 5

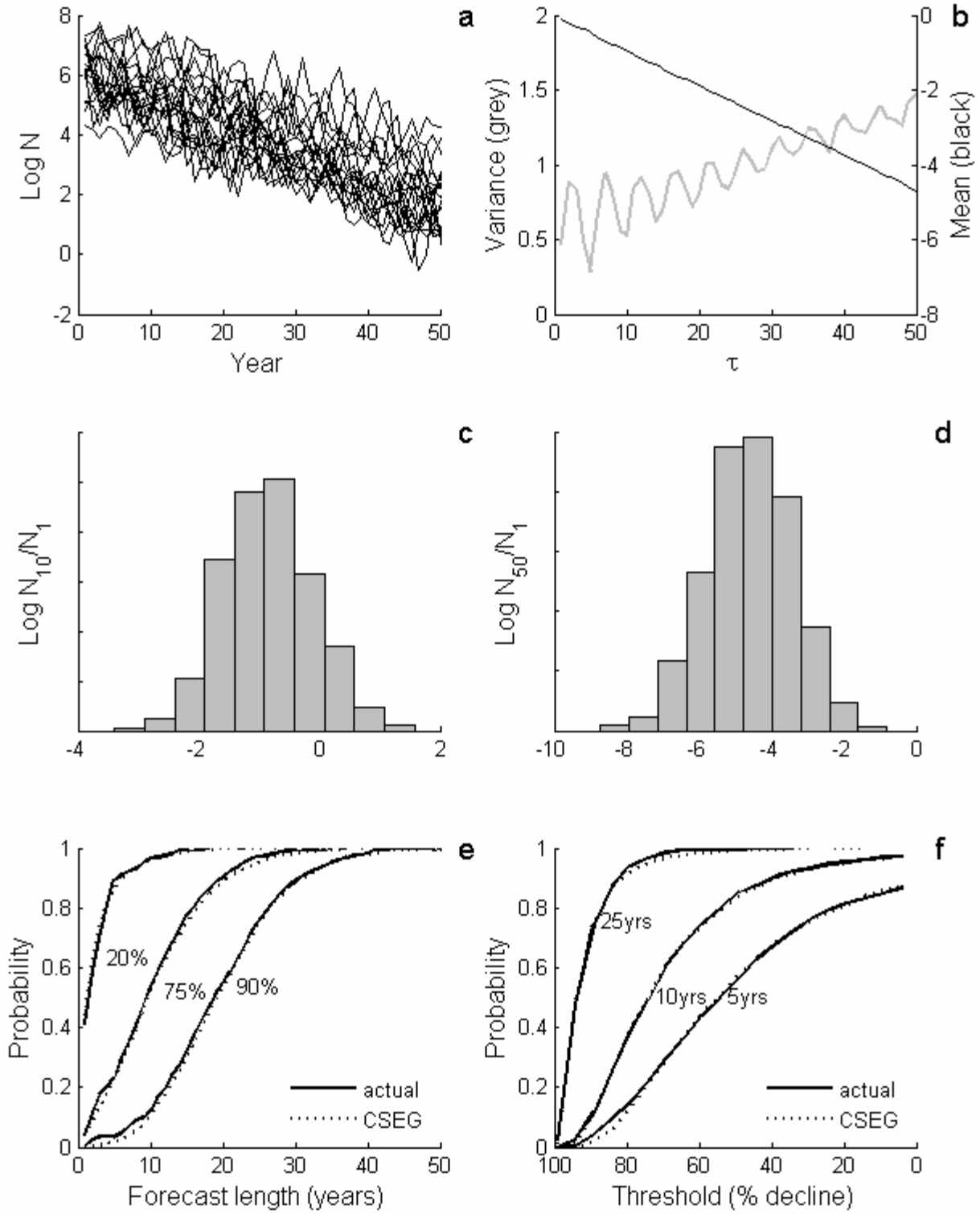
a
b
Log N
Year
Variance (grey)
Mean (black)
τ
c
d
Log N10/N1
Log N50/N1
e
f
Probability
20%
75%
90%
actual
CSEG
Forecast length (years)
25yrs
10yrs
5yrs
Threshold (% decline)

Fig. 6

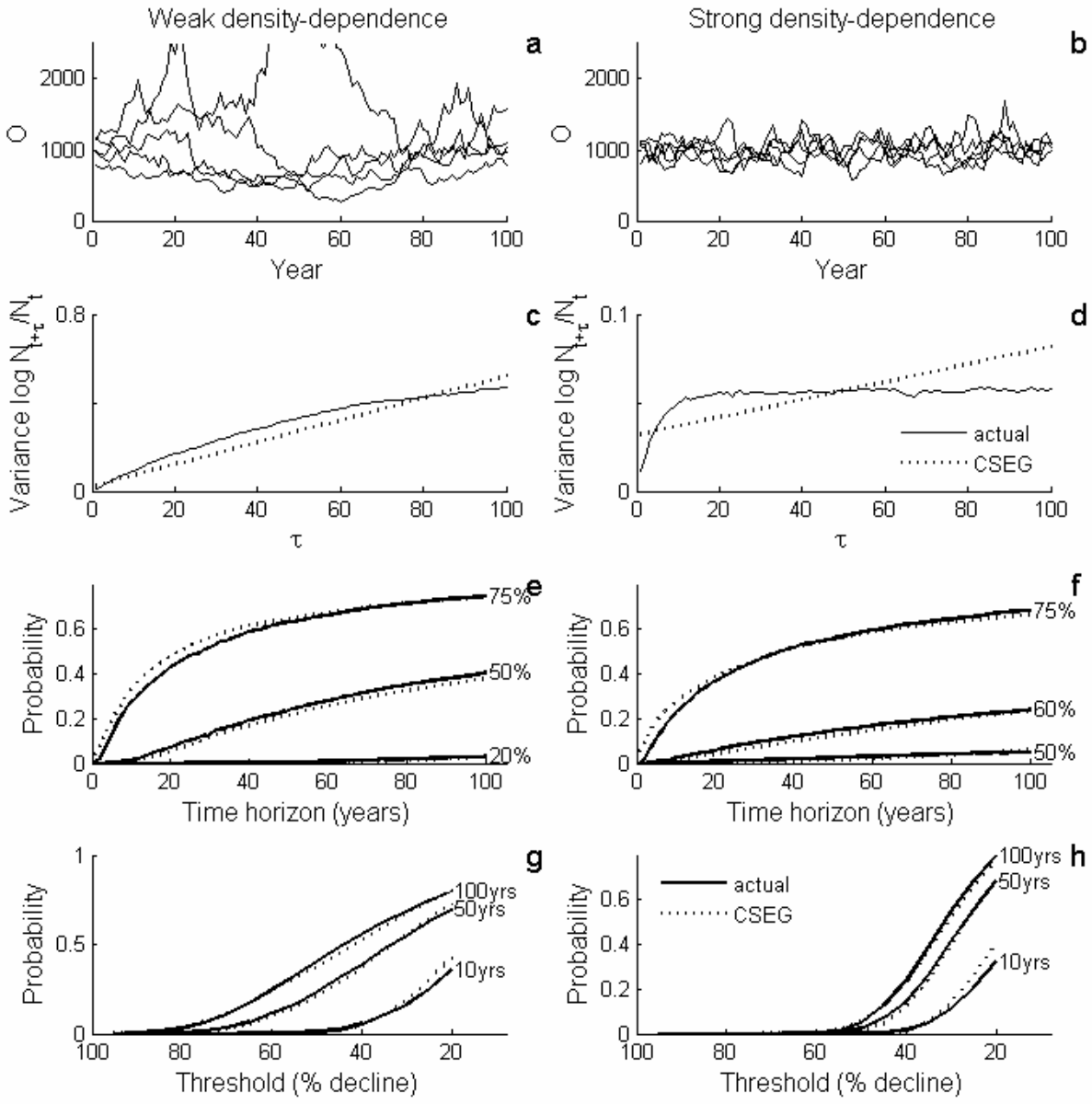
Weak density-dependence
Strong density-dependence
a
b
c
d
e
f
g
h
N
Year
Variance log $N_{t+\tau}/N_t$
τ
actual
CSEG
Probability
Time horizon (years)
75%
50%
20%
60%
100yrs
50yrs
10yrs
Threshold (% decline)

Fig. 7

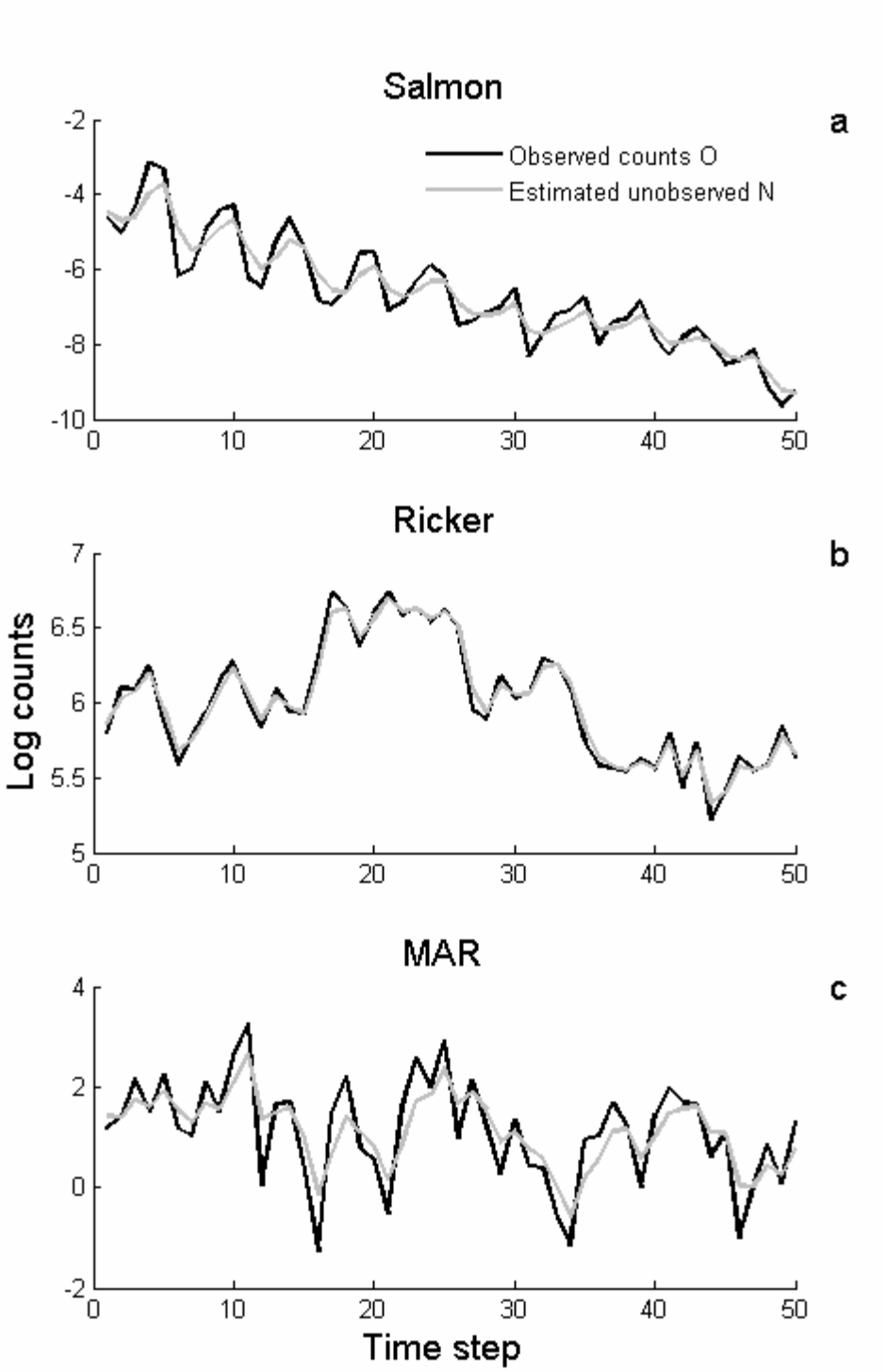
Salmon
a
Observed counts O
Estimated unobserved N
-2
-4
-6
-8
-10
0
10
20
30
40
50
Ricker
b
Log counts
7
6.5
6
5.5
5
MAR
c
4
2
0
-2
Time step

Fig. 8

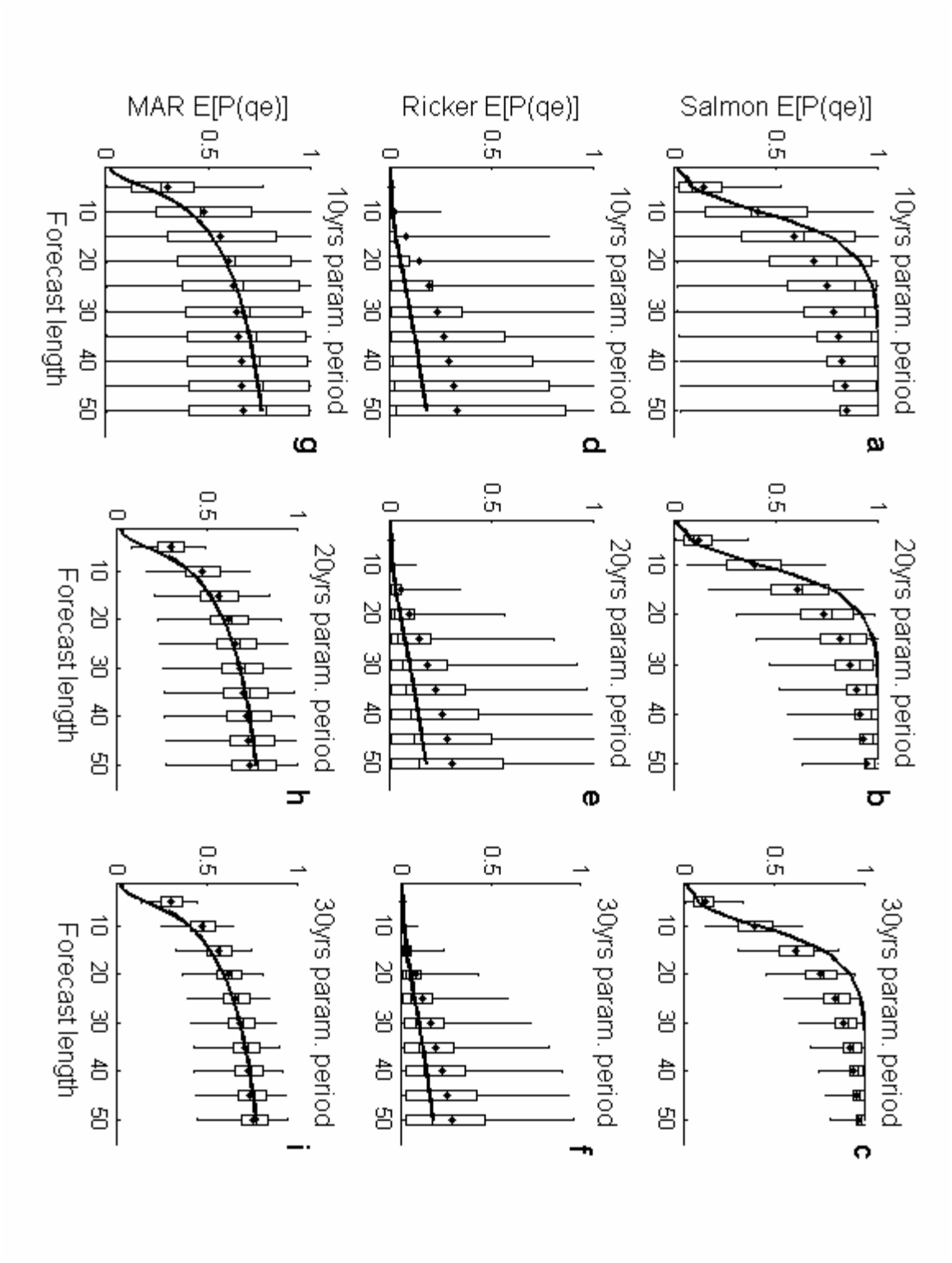
Salmon E[P(qe)]
Ricker E[P(qe)]
MAR E[P(qe)]
10yrs param. period
20yrs param. period
30yrs param. period
Forecast length
a
b
c
d
e
f
g
h
i

Fig. 9

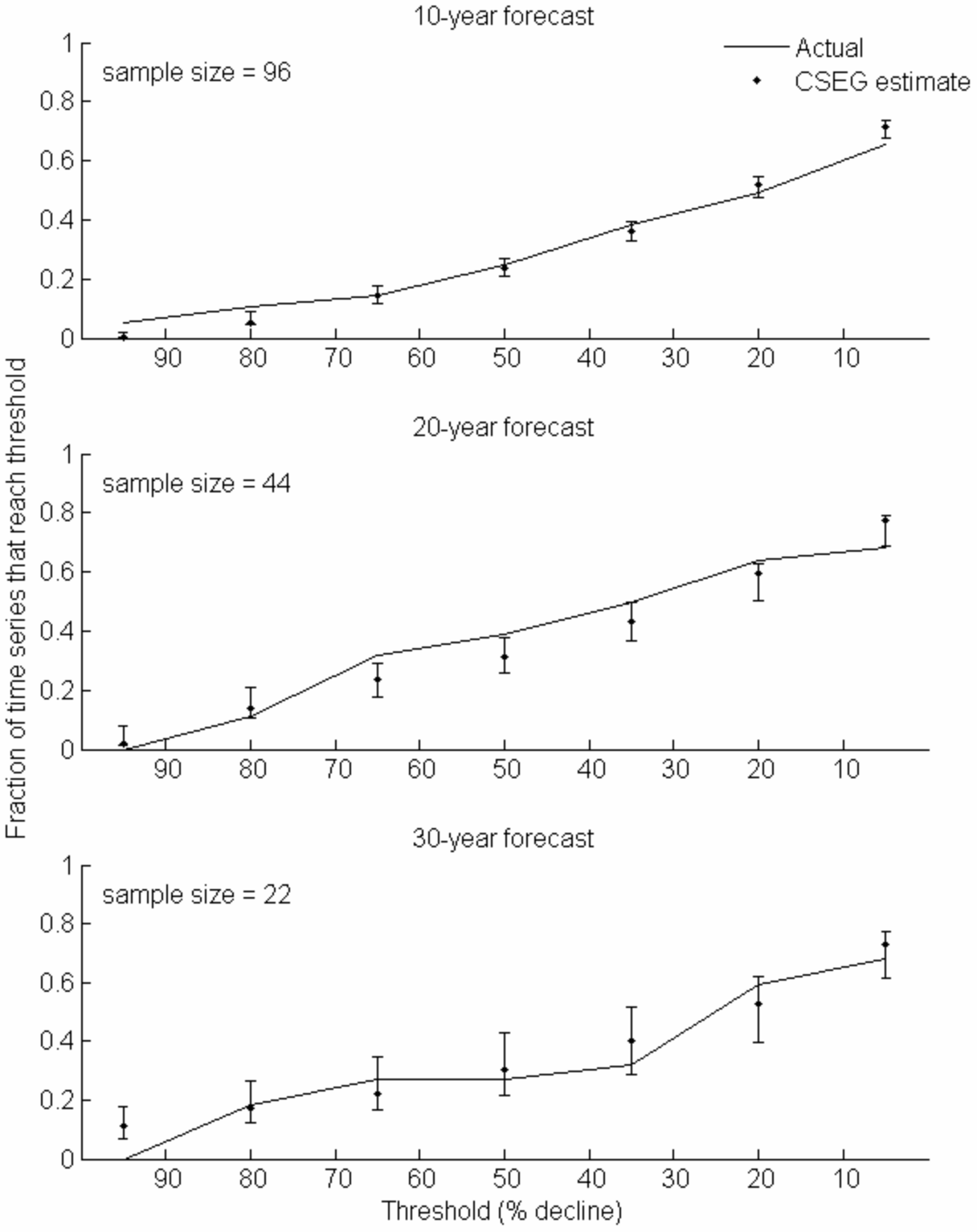
10-year forecast
sample size = 96
Actual
CSEG estimate
20-year forecast
sample size = 44
30-year forecast
sample size = 22
Fraction of time series that reach threshold
Threshold (% decline)
0
0.2
0.4
0.6
0.8
1
90
80
70
60
50
40
30
20
10

Fig. 10

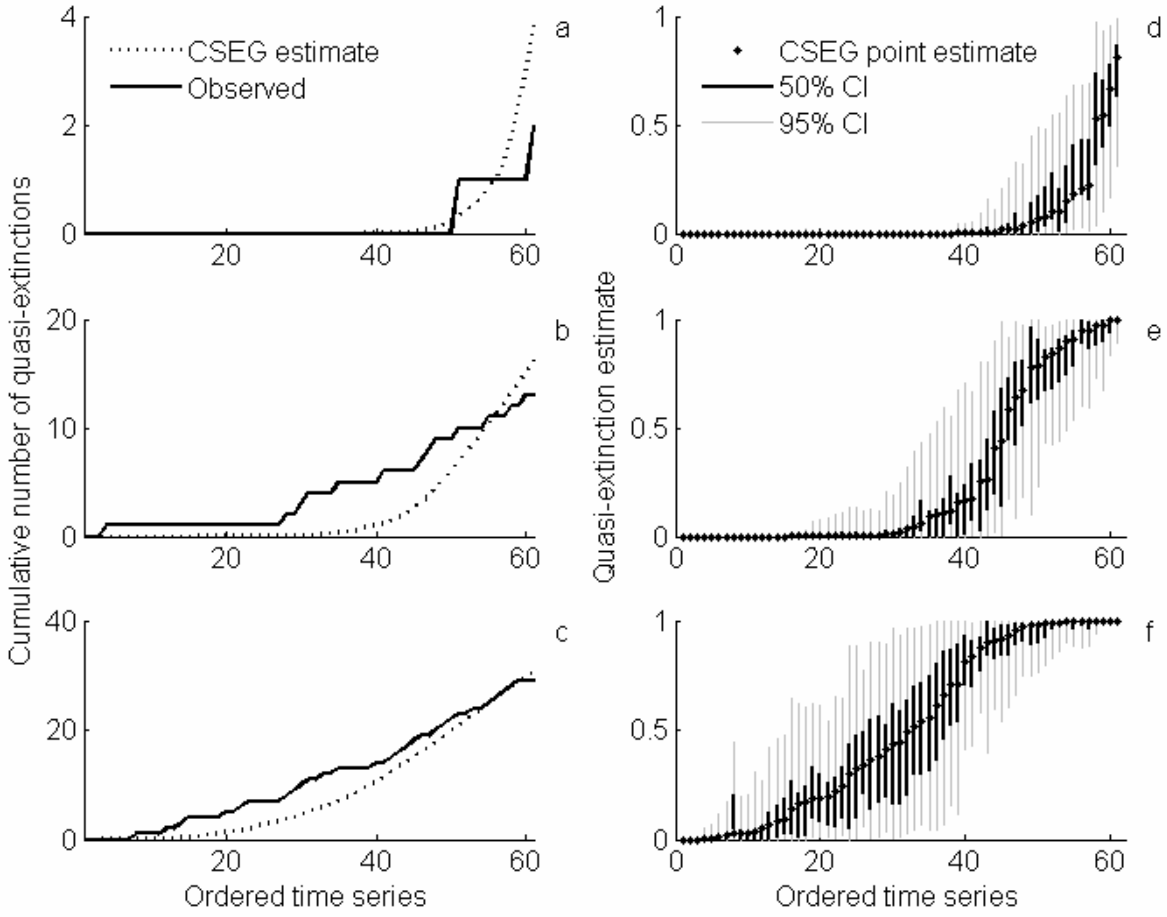
CSEG estimate
Observed
a
b
c
Cumulative number of quasi-extinctions
Ordered time series
CSEG point estimate
50% CI
95% CI
d
e
f
Quasi-extinction estimate
Ordered time series

Table S1. Summary of population time series used in cross-validation analyses. Only surveys that represented an index of an entire distinct population or subpopulation were used. Breeding ground surveys from single colonies were used when the species showed high year-to-year site fidelity or the colony was a representative index of the population. The references show the original references for the data. Many of the time series were updated by direct contact with the authors or government agencies involved. If the species is listed above the LC (least concern) status on the IUCN Red List, that is noted first in the Status column. If the study population is listed separately in the country or region where the censuses take place, that is listed next. Explanation of the status level is given in the footnote. Unit of census refers to the segment of the population that is censused. 'Total population' does not mean that the total population is counted (in all except two cases, the surveys are index counts of some sort), but rather that the count includes all ages and sexes.

Common Name	Species	Status in 2006*	Taxonomic Class	Location of Study Population	Length (yrs)	# of Counts	Type of Census	References
American Woodcock	*Scolopax minor*		Aves	Eastern region, U.S.	39	39	Total Population	Kelley & Rau (2006)
Antarctic Fulmar	*Fulmarus glacialoides*		Aves	Pointe Geologie Archipelago, Antarctica	36	36	Total Population	Jouventin & Weimerskirch (1991)
Attwater's Prairie Chicken	*Tympanuchus cupido attwateri*	EN USA	Aves	Coastal Prairie, Louisiana and Texas	59	30	Total Population	Peterson & Silvy (1996)
Curlew	*Numenius arquata*	A UK	Aves	'The Hille', Lancashire, UK	32	32	Territories per km	Fuller, *et al.* (2002)
Bald Eagle	*Haliaeetus leucocephalus*	T USA	Aves	Florida	31	31	Occupied Territories	Bureau of Wildlife Diversity Conservation (2003)
Buller's Albatross	*Thalassarche bulleri*	VU IUCN	Aves	West Coast, North Island, NZ	35	35	Beach Carcass Cnt/km	Ornithological Society of NZ, Beach Patrol Database
Common Eider	*Somateria mollissima*		Aves	Wadden Sea Coast, Germany	37	34	Breeding Pairs	Becker (1991)
Emperor Penguin	*Aptenodytes forsteri*		Aves	Pointe Geologie Archipelago, Antarctica	37	36	Breeding Pairs	Micol & Jouventin (2000)

Common Name	Species	Status in 2006*	Taxonomic Class	Location of Study Population	Length (yrs)	# of Counts	Type of Census	References
Great Tit	*Parus major*		Aves	Wytham Wood, UK	31	31	Total Population	Saether, *et al.* (1998)
Grey-headed Albatross	*Thalassarche chrysostoma*	VU IUCN	Aves	West Coast, North Island, NZ	35	35	Beach Carcass Cnt/km	Ornithological Society of NZ, Beach Patrol Database
Grey Heron	*Ardea herodias*		Aves	England and Wales	50	50	Occupied Nests	Stafford (1971) Reynolds (1974) Reynolds (1979)
Kirtland's Warbler	*Dendroica kirtlandii*	VU IUCN EN USA	Aves	northern half of Michigan's lower peninsula	33	33	Singing Males	Dennis, *et al.* (1991) Solomon (1998)
Kittiwake	*Rissa tridactyla*	A UK	Aves	North Shields, Tyne and Wear, UK	34	34	Nests with Eggs	Coulson & Thomas (1985)
Lapwing	*Vanellus vanellus*	A UK	Aves	'The Hille', Lancashire, UK	32	32	Territories per km	Fuller, *et al.* (2002)
Light-mantled Albatross	*Phoebetria palpebrata*	NT IUCN 5 NZ	Aves	West Coast, North Island, NZ	35	35	Beach Carcass Cnt/km	Ornithological Society of NZ, Beach Patrol Database
Meadow Pipit	*Anthus pratensis*	A UK	Aves	'The Hille', Lancashire, UK	32	32	Territories per km	Fuller, *et al.* (2002)
Mute Swan	*Cygnus olor*	A UK	Aves	Thames River, UK	150	138	Total Population	Cramp (1972)
New Zealand Shore Plover	*Thinornis novaeseelandiae*	EN IUCN 1 NZ	Aves	South East Island, Chatham Islands, NZ	39	20	Total Adults	Davis (1994) Department of Conservation (2001)
Peregrine Falcon	*Falco peregrinus*	A UK	Aves	Cumbria, UK	34	34	Breeding Pairs	Horne & Fielding (2002)
Puerto Rican Parrot	*Amazona vittata*	CR IUCN EN USA	Aves	Puerto Rico	32	21	Total Population	Snyder, *et al.* (1987) U.S. Fish and Wildlife Service (1999)
Reed Bunting	*Emberiza schoeniclus*	A UK	Aves	'The Hille', Lancashire, UK	32	32	Territories per km	Fuller, *et al.* (2002)

Common Name	Species	Status in 2006*	Taxonomic Class	Location of Study Population	Length (yrs)	# of Counts	Type of Census	References
Red Kite	*Milvus milvus*	A UK	Aves	Wales	49	41	Total Population	Davis & Newton (1981)
Red-Crowned Crane	*Grus japonesis*	EN IUCN	Aves	Hokkaido, Japan	36	36	Total Population	Masatomi (1987)
Roseate Terns	*Sterna dougallii*	R UK	Aves	main colonies in Ireland, Britain, and France	35	35	Breeding Pairs	Cabot (1996)
Greater Sage-Grouse	*Centrocercus urophasianus*	Petitioned US	Aves	Washington	34	34	Total Population	Stinson, *et al.* (2004)
Seychelles Magpie Robin	*Copsychus seychellarum*	CR IUCN	Aves	Frigate Is, Seychelles	35	22	Total Population	Komdeur (1996)
Sharptailed Grouse	*Tympanuchus phasianellus*	SC US	Aves	Washington	30	30	Total Population	Hays, *et al.* (1998)
Skylark	*Alauda arvensis*	A UK	Aves	'The Hille', Lancashire, UK	32	32	Territories per km	Fuller, *et al.* (2002)
Snipe	*Gallinago gallinago*	A UK	Aves	'The Hille', Lancashire, UK	32	32	Territories per km	Fuller, *et al.* (2002)
Sooty Shearwater	*Puffinus griseus*	NT IUCN 5 NZ	Aves	New Zealand	39	39	Carcass surveys	Scofield & Christie (2002)
South Polar Skua	*Stercorarius maccormicki*		Aves	Pointe Geologie Archipelago, Antarctica	34	31	Territories	Micol & Jouventin (2000)
Southern Giant Petrel	*Macronectes giganteus*	VU IUCN	Aves	Pointe Geolgie Archipelago, Antarctica	39	36	Fledged chicks	Micol & Jouventin (2000)
Trumpeter Swan	*Cygnus buccinator*	VU1 Canada	Aves	RMP/tri-state flock, Rocky Mountains, US & Canada	33	25	Total Population	U.S. Fish and Wildlife Service (2004)

Common Name	Species	Status in 2006*	Taxonomic Class	Location of Study Population	Length (yrs)	# of Counts	Type of Census	References
Trumpeter Swan	*Cygnus buccinator*	Petitioned US	Aves	RMP/Canada flock, Rocky Mountains, US & Canada	33	25	Total Population	U.S. Fish and Wildlife Service (2004)
Twite	*Carduelis flavirostris*	A UK	Aves	'The Hille', Lancashire, UK	32	32	Territories per km	Fuller, *et al.* (2002)
White Heron	*Egretta alba modesta*	1 NZ	Aves	Waitangiroto River, New Zealand	51	45	Nests	Miller (2001)
White Stork	*Ciconia ciconia*	2 SPEC	Aves	Baden-Wurttenberg, Germany	39	39	Breeding Pairs	Bairlein (1991) Newton (1998)
White Stork	*Ciconia ciconia*	2 SPEC	Aves	Oldenburg/NW Germany	61	61	Breeders	Bairlein (1991)
White-capped Albatross	*Thalassarche steadi*	NT IUCN	Aves	West Coast, North Island, NZ	35	35	Beach Carcass Cnt/km	Ornithological Society of NZ, Beach Patrol Database
Whooping Crane	*Grus americana*	EN IUCN EN USA	Aves	Arkansas, Texas	66	66	Total Population	Dennis, *et al.* (1991)
African Elephant	*Loxodonta africana*	EN IUCN	Mammalia	Addo National Park, South Africa	69	69	Total Population	Whitehouse & Hall-Martin (2000)
Alpine Ibex	*Capra ibex*		Mammalia	Gran Paradiso National Park, Italy	45	45	Total Population	Jacobson, *et al.* (2004)
California Gray Whale	*Eschrichtium robustus*	MMPA	Mammalia	California	46	24	Total Population	Gerber, *et al.* (1999)
Columbian White-tailed Deer	*Odocoileus virginianus leucurus*	EN USA[3]	Mammalia	Douglas County, Oregon	31	31	Total Population	U.S. Fish and Wildlife Service (2003) U.S. Fish and Wildlife Service (2006)
Grizzly Bear	*Ursus arctos horribilis*	T USA	Mammalia	Yellowstone National Park	43	43	Adult Females	Eberhardt, *et al.* (1986) Haroldson (2004)
Hawaiian Monk Seal	*Monachus shauinslandi*	EN IUCN EN USA	Mammalia	Hawaiian Islands minus Midway	46	31	Entire Population (almost)	Gilmartin & Eberhardt (1995) Ragen & Lavigne (1999)

Common Name	Species	Status in 2006*	Taxonomic Class	Location of Study Population	Length (yrs)	# of Counts	Type of Census	References
Musk Ox	*Ovibos moschatus*		Mammalia	Nunivak Island, Alaska	33	25	Total Population	Spencer & Lensink (1970)
Northern Fur Seal	*Callorhinus ursinus*	VU IUCN VU USA	Mammalia	St. Paul Island, Alaska	96	94	Bull Count	National Marine Mammal Laboratory, unpublished data
Northern Fur Seal	*Callorhinus ursinus*	VU IUCN VU USA	Mammalia	St. George Island, Alaska	96	96	Bull Count	National Marine Mammal Laboratory, unpublished data
Northern Fur Seal	*Callorhinus ursinus*	VU IUCN VU USA	Mammalia	St. George Island, Alaska	53	46	Pups	York & Hartley (1981) York (1985) York, *et al.* (2000)
Northern Fur Seal	*Callorhinus ursinus*	VU IUCN VU USA	Mammalia	St. Paul Island, Alaska	53	46	Pups	York & Hartley (1981) York (1985) York, *et al.* (2000)
Northern Fur Seal	*Callorhinus ursinus*	VU IUCN VU USA	Mammalia	San Miguel Island, California	30	30	Pups	York & Hartley (1981) York (1985) York, *et al.* (2000)
Northern Resident Killer Whale	*Orcinus orca*	EN Canada	Mammalia	Pacific Northwest, US & Canada	31	31	Total Population	Wiles (2004)
Pronghorn Antelope	*Antelocapra americana*		Mammalia	Yellowstone National Park	33	32	Spring Population	Keating (2002)
Pronghorn Antelope	*Antelocapra americana*		Mammalia	Northern Arizona	53	53	Total Population	U.S. Fish and Wildlife Service, unpublished data
Southern Resident Killer Whale	*Orcinus orca*	EN USA	Mammalia	Pacific Northwest, US & Canada	31	31	Entire Population	Wiles (2004)
Vancouver Island Marmot	*Marmota vancouverensis*	EN IUCN	Mammalia	Vancouver Island, Canada	30	27	Total Population	Janz, *et al.* (2000)
Weddell Seal	*Leptonychotes weddellii*		Mammalia	McMurdo Sound, Antartica	38	38	Pups	Cameron & Siniff (2004) Cameron (2001)
Wildebeest	*Connochaetes taurinus*	CD IUCN	Mammalia	Ngorongoro Crater, Tanzania	30	22	Total Population	Runyoro, *et al.* (1995)

Common Name	Species	Status in 2006*	Taxonomic Class	Location of Study Population	Length (yrs)	# of Counts	Type of Census	References
Western Swamp Tortoise	*Pseudemydura umbrina*	CR IUCN CR AU	Reptilia	Ellen Brook Reserve, W. Australia	37	37	Total Population	Burbidge & Kuchling (2004)
Western Swamp Tortoise	*Pseudemydura umbrina*	CR IUCN CR AU	Reptilia	Twin Swamps Reserve, W. Australia	31	31	Total Population	Burbidge & Kuchling (2004)

*Status: IUCN: EX (extinct), CR (critically endangered), EN (endangered), VU (vulnerable), T (threatened), CD (conservation dependent), NT (near threatened). USA: EN (endangered), T (threatened), VU (vulnerable), SC (special concern). UK: R (Red-listed), A (Amber-listed), BCI (Bird of Conservation Importance, Joint Nature Conservation Committee). AU: CR (critically endangered), VU (vulnerable). NZ: 1 (nationally critical), 5 (gradual decline). SPEC, Species of European Concern: 2 (depleted). MMPA (covered under the U.S. Marine Mammal Protection Act).
1 Delisted 1996

2 The Wood Turtle is listed as endangered, threatened, or special concern at the state level throughout its range in the U.S.
3 The Douglas County DPS was delisted in 2003.